

Journal of Visualized Experiments

Probing metabolism and viscosity of cancer cells using fluorescence lifetime imaging microscopy --Manuscript Draft--

Article Type:	Methods Article - Author Produced Video
Manuscript Number:	JoVE62708R2
Full Title:	Probing metabolism and viscosity of cancer cells using fluorescence lifetime imaging microscopy
Corresponding Author:	Marina V. Shirmanova, Ph.D. Privolzhsky Research Medical University: Privolzhskij issledovatel'skij medicinskij universitet Nizhny Novgorod, no RUSSIAN FEDERATION
Corresponding Author's Institution:	Privolzhsky Research Medical University: Privolzhskij issledovatel'skij medicinskij universitet
Corresponding Author E-Mail:	shirmanovam@gmail.com
Order of Authors:	Liubov Shimolina Maria Lukina Vladislav Shcheslavskiy Vadim Elagin Varvara Dudenkova Nadezhda Ignatova Marina Kuimova Marina V. Shirmanova, Ph.D.
Additional Information:	
Question	Response
Please specify the section of the submitted manuscript.	Cancer Research
Please indicate whether this article will be Standard Access or Open Access.	Standard Access (\$1400)
Please confirm that you have read and agree to the terms and conditions of the author license agreement that applies below:	I agree to the UK Author License Agreement (for UK authors only)
Please provide any comments to the journal here.	This manuscript is submitted to a Methods Collection "Multimodal Imaging of Cancer" by the invitation from Dr. Anna N. Yaroslavsky
Please confirm that you have read and agree to the terms and conditions of the video release that applies below:	I agree to the Video Release

TITLE:

Probing Metabolism and Viscosity of Cancer Cells using Fluorescence Lifetime Imaging Microscopy

AUTHORS AND AFFILIATIONS:

Liubov Shimolina¹, Maria Lukina¹, Vladislav Shcheslavskiy^{1,2}, Vadim Elagin¹, Varvara Dudenkova¹, Nadezhda Ignatova¹, Marina K. Kuimova³, Marina Shirmanova¹

¹Institute of Experimental Oncology and Biomedical Technologies, Privolzhsky Research Medical University, Minin and Pozharsky Square, 10/1, 603005 Nizhny Novgorod, Russia

²Becker & Hickl GmbH, Nunsdorfer Ring 7-9, 12277 Berlin, Germany

³Department of Chemistry, Imperial College London, South Kensington, SW7 2AZ London, United Kingdom

Email Addresses of co-Authors:

Liubov Shimolina	(shimolina.l.e@gmail.com)
Maria Lukina	(kuznetsova.m.m@yandex.ru)
Vladislav Shcheslavskiy	(vis@becker-hickl.de)
Vadim Elagin	(elagin.vadim@gmail.com)
Varvara Dudenkova	(oranne@mail.ru)
Nadezhda Ignatova	(n.i.evteeva@gmail.com)
Marina K. Kuimova	(m.kuimova@imperial.ac.uk)
Marina Shirmanova	(shirmanovam@gmail.com)

Email Address of Corresponding Author:

Marina Shirmanova (shirmanovam@gmail.com)

KEYWORDS:

fluorescence lifetime imaging microscopy, metabolism, fluorescent metabolic co-factors, NADH, flavins, microviscosity, fluorescent molecular rotor, cancer cells

SUMMARY:

Here, we demonstrate the use of fluorescence lifetime imaging microscopy (FLIM) to sequentially image cellular metabolism and plasma membrane viscosity in live cancer cell culture. Metabolic assessments are performed by detecting endogenous fluorescence. Viscosity is measured using a fluorescent molecular rotor.

ABSTRACT:

Viscosity is an important physical property of a biological membrane, as it is one of the key parameters for the regulation of morphological and physiological state of living cells. Plasma membranes of tumor cells are known to have significant alterations in their composition, structure, and functional characteristics. Along with dysregulated metabolism of glucose and lipids, these specific membrane properties help tumor cells to adapt to the hostile microenvironment and develop resistance to drug therapies. Here, we demonstrate the use of

fluorescence lifetime imaging microscopy (FLIM) to sequentially image cellular metabolism and plasma membrane viscosity in live cancer cell culture. Metabolic assessments are performed by detecting fluorescence of endogenous metabolic co-factors, such as reduced nicotinamide adenine dinucleotide NAD(P)H and oxidized flavins. Viscosity is measured using a fluorescent molecular rotor, a synthetic viscosity-sensitive dye, with a strong fluorescence lifetime dependence on the viscosity of the immediate environment. In combination, these techniques enable us to better understand the links between membrane state and metabolic profile of cancer cells and to visualize the changes induced by chemotherapy.

INTRODUCTION:

Malignant transformation of cells is accompanied by multiple alterations in their morphological and physiological state. Rapid and uncontrolled growth of cancer cells requires fundamental re-organization of biochemical pathways responsible for energy production and biosynthesis. The characteristic hallmarks of cancer metabolism are enhanced rate of glycolysis, even under the normal oxygen concentrations (the Warburg effect), the use of amino acids, fatty acids, and lactate as alternative fuels, high ROS production in the presence of high antioxidant levels, and increased biosynthesis of fatty acids^{1,2}. It is now appreciated that cancer cell metabolism is highly flexible, which allows them to adapt to the unfavorable and heterogeneous environment and provides an additional survival advantage³.

Altered metabolism supports the specific organization and composition of membranes of tumor cells. The lipid profile of the plasma membrane in cancer cells quantitatively differs from the non-cancerous cells. The main changes in the lipidome are the increased level of phospholipids including phosphatidylinositol, phosphatidylserine, phosphatidylethanolamine and phosphatidylcholine, the decreased level of sphingomyelin, increased amount of cholesterol, and a lower degree of unsaturation of fatty acids, to name a few⁴⁻⁶. Therefore, physical properties of the membrane, such as membrane viscosity, the inverse of fluidity, inevitably change. Since viscosity determines the permeability of biological membranes and controls the activity of membrane-associated proteins (enzymes, transporters, receptors), its homeostatic regulation is vital for cell functioning. At the same time, the modification of viscosity through the adjustment of membrane lipid profile is important for cell migration/invasion and survival upon conditional changes.

Fluorescence lifetime imaging microscopy (FLIM) has emerged as a powerful approach for the non-invasive assessment of multiple parameters in living cells, using endogenous fluorescence or exogenous probes⁷. FLIM is commonly realized on a multiphoton laser scanning microscope, which provides (sub)cellular resolution. Being equipped with the time-correlated single-photon counting (TCSPC) module, it enables time-resolved measurements of fluorescence with high accuracy⁸.

Probing of cellular metabolism by FLIM is based on the fluorescence measurement of endogenous co-factors of dehydrogenases, the reduced nicotinamide adenine dinucleotide (phosphate) NAD(P)H and oxidized flavins - flavin adenine dinucleotide FAD and flavin mononucleotide FMN, that act as electron carriers in a number of biochemical reactions^{7,9,10}.

The detected fluorescence of NAD(P)H is from NADH and its phosphorylated form, NADPH, as they are spectrally almost identical. Typically, fluorescence decays of NAD(P)H and flavins fit to a bi-exponential function. In the case of NAD(P)H, the first component ($\sim 0.3\text{--}0.5$ ns, $\sim 70\%\text{--}80\%$) is attributed to its free state, associated with glycolysis, and the second component ($\sim 1.2\text{--}2.5$ ns, $\sim 20\%\text{--}30\%$) to its protein-bound state, associated with mitochondrial respiration. In the case of flavins, the short component ($\sim 0.3\text{--}0.4$ ns, $\sim 75\%\text{--}85\%$) can be assigned to the quenched state of FAD and the long component ($\sim 2.5\text{--}2.8$ ns, $\sim 15\%\text{--}25\%$) to unquenched FAD, FMN, and riboflavin. Alterations in the relative levels of glycolysis, glutaminolysis, oxidative phosphorylation, and fatty acid synthesis result in the changes in the short- and long lifespan fractions of the co-factors. Additionally, the fluorescence intensity ratio of these fluorophores (the redox ratio) reflects the cellular redox status and is also used as a metabolic indicator. Although the redox ratio presents a simpler metric, compared with fluorescence lifetime, in terms of data acquisition, FLIM is advantageous to estimate NAD(P)H and FAD, because fluorescence lifetime is an intrinsic characteristic of the fluorophore and almost not influenced by such factors as excitation power, photobleaching, focusing, light scattering and absorption, especially in tissues, unlike the emission intensity.

One of the convenient ways to map viscosity in living cells and tissues at the microscopic level is based on the use of fluorescent molecular rotors, small synthetic viscosity-sensitive dyes, in which fluorescence parameters strongly depend on the local viscosity^{11,12}. In a viscous medium, the fluorescence lifetime of the rotor increases due to the slowing down of the intramolecular twisting or rotation. Among molecular rotors, the derivatives of boron dipyrromethene (BODIPY) are well suited for sensing viscosity in biological systems as they have a good dynamic range of fluorescence lifetimes in physiological range of viscosities, temperature independence, monoexponential fluorescence decays that allow straightforward data interpretation, sufficient water-solubility and low cytotoxicity^{13,14}. Quantitative assessments of microviscosity using BODIPY-based rotors and FLIM has been previously demonstrated on cancer cell *in vitro*, multicellular tumor spheroids and mouse tumor *in vivo*^{15,16}.

Here, we present a detailed description of sequential probing methodologies for studying cellular metabolism and plasma membrane viscosity in cancer cells *in vitro* by FLIM. To avoid contamination of the relatively weak endogenous fluorescence with the fluorescence of the BODIPY-based rotor, imaging of the same layer of cells is performed sequentially with the fluorescence of NAD(P)H and FAD imaged first. Fluorescence lifetimes of the co-factors are measured in the cytoplasm, and the fluorescence lifetime of the rotor is measured in the plasma membranes of cells by the manual selection of corresponding zones as regions of interest. The protocol was applied to correlate metabolic state and viscosity for different cancer cell lines and to assess the changes after chemotherapy.

In this article, we present a detailed protocol of methodologies of optical imaging of cellular metabolism and mapping viscosity of plasma membrane of cultured cancer cells by FLIM. The protocol for FLIM sample preparation does not differ from that for confocal fluorescence microscopy. Once data has been acquired, the main task is to extract the fluorescence lifetime from the raw data. The performance of the protocol is demonstrated using HCT116 (human

colorectal carcinoma), CT26 (murine colon carcinoma), HeLa (human cervical carcinoma), and huFB (human skin fibroblasts) cells.

PROTOCOL:

1. Description of the minimal setup to perform FLIM

1.1. To perform this experiment, ensure the required setup is available: an inverted confocal microscope, a pulsed laser, typically a ps or fs, with the synchronization signal, a fast photon counting detector (time response 150 ps) and photon counting electronics, available output and input ports for the detector and the laser, respectively, on the microscope, the scan clock pulses from the microscope scan controller, the scan head of the microscope with the laser beam combiners and the main dichroic beam splitters suitable for the wavelength of the laser used for FLIM.

1.2. If two-photon excitation is used for FLIM, ensure the microscope contains the NDD port.

1.3. For mammalian cell studies, especially for long-term experiments, ensure having a CO₂ incubator maintained at the desired temperature.

NOTE: For the system used in this experiment, see **Table of Materials**.

2. Preparation of cells for microscopy

2.1. Grow the cells routinely in an incubator at 37 °C with 5% CO₂ and a humid atmosphere.

2.2. For microscopy, prepare the cell suspension in a complete culture medium at the concentration of 1×10^6 cells/mL.

NOTE: The cell concentrations and media conditions are cell dependent. The number of cells used for seeding and the incubation time should be adapted to obtain 70%–80% confluence in the microscopic dish.

2.3. Seed the cells on glass-bottom 35 mm cell culture dishes (1×10^5 cells in 100 µL per dish) using a 200 µL automatic pipette.

NOTE: Use gridded glass-bottom dishes for the cells seeding to monitor cells in the same microscopic fields of view in dynamics.

2.3.1. During the manual seeding, ensure that the pipette tip does not scratch the bottom or the sides of the dish to avoid damaging the bottom.

2.4. Place the dish in the CO₂ incubator (37 °C, 5% CO₂, humid atmosphere) and incubate the cells for 24 h.

2.5. After 24 h, remove the dish from the incubator and check the cells' morphology and confluence under the light microscope. If the cells did not reach about 80% confluency, incubate for an additional 24 h.

2.6. Gently remove the old medium from the dish using a 1,000 μ L automatic pipette and add 2 mL of DMEM medium without phenol red (e.g., DMEM Life or FluoroBrite).

NOTE: Different culture media can be used for imaging. Avoid phenol red in the medium when using cells for microscopy.

2.7. Place the dish in the incubator for 60–120 min to allow for the adaptation of cells.

3. FLIM of metabolic co-factors

3.1. Place the glass-bottom dish with the cells (from step 2.7) on the microscope stage.

3.2. Click on the **Locate** tab in the laser scanning microscope software (e.g., ZEN - ZEISS Efficient Navigation), and then click on **Transmission Light (TL)** to switch the light on.

3.3. Find the focal plane of the sample by viewing through the eyepiece on the central slice level of the cells, where a square is maximally occupied by cells (at magnification 40x).

3.4. Click on the **OFF** button to switch the light off.

3.5. Open the **Acquisition** tab. To obtain transmission and autofluorescence intensity images of endogenous NAD(P)H, enter the following settings: **Excitation wavelength**: two-photon mode 750 nm, **Registration range**: 450–490 nm, **Laser power**: 5% (~6 mW), **Image size**: 1024 x 1024 pixels.

NOTE: The choice of the excitation wavelength and registration range is based on the spectral characteristics (maximum excitation and maximum emission) of NAD(P)H¹⁷.

3.5.1. Use an oil immersion objective lens C Plan-Apochromat 40x/1.3 NA for the image acquisition.

3.6. Press the **Snap** button and save the image in ZEN format.

3.7. To obtain the transmission and autofluorescence intensity images of FAD, change the **Excitation Wavelength** to 900 nm. Set the **Registration Range**: 500–550 nm, **Laser power**: 9% (~6 mW), and **Image Size**: 1024 x 1024 pixels.

NOTE: The choice of the excitation wavelength and registration range is based on the spectral characteristics (maximum excitation and maximum emission) of FAD¹⁸.

3.7.1. Use an oil immersion objective lens C Plan-Apochromat 40x/1.3 NA for image acquisition.

3.8. Press the **Snap** button and save the image in ZEN format.

3.9. For NAD(P)H, set the parameters as described in step 3.5 in the laser scanning microscope software. Change the **Image Size** to 256 x 256 pixels.

3.10. Enter the following parameters in the menu of SPCM (Single Photon Counting Modules) Operating software of FLIM module: **Collection Time:** 60 s; **TAC Range:** 5.00E-8; **CFD Limit Low:** -29.41; **ADC Resolution:** 256, **Image Size:** 256 x 256 pixels.

3.11. Scan the sample for 60 s, stop scanning and save the obtained FLIM image of NAD(P)H.

3.12. Check the obtained FLIM data. For this, **Open** the raw data in the image software, select a pixel in the cell's cytoplasm by placing the cursor over it and analyze the fluorescence decay in this pixel. Pixel intensities should be $\geq 3,000$ photons per decay curve at binning 1.

NOTE: If the number of photons is below 3,000, increase the laser power or image collection time, while controlling the morphology of cells and photon-counting rate. Typically, if the drop in the count rate exceeds 10% of the initial value, photobleaching takes place.

3.13 Repeat steps 3.3–3.10 to record FLIM images from different fields of view.

3.14 For FAD, set the parameters as described in step 3.7 in the laser scanning microscope's software. Change the image size to 256 x 256 pixels.

3.15 Enter the following parameters in the menu of SPCM (Single Photon Counting Modules) Operating software of FLIM module: **Collection time:** 60 s; **TAC Range:** 5.00E-8; **CFD Limit Low:** -29.41; **ADC Resolution:** 256, **Image Size:** 256 x 256 pixels.

3.16 Scan the sample for 60 s. Stop scanning and save the obtained FLIM image of FAD.

NOTE: The parameters indicated in steps 3.10 and 3.15 are specific for the electronics and the detector used.

3.17 Check the obtained data as described in step 3.12.

4. Staining of cells with the fluorescent molecular rotor

NOTE: The cells are imaged in the fluorescent molecular rotor solution without washing at room temperature ($\sim 20^\circ\text{C}$) to slow down the internalization of the rotor. Membrane viscosity is temperature dependent, as demonstrated in our previous works^{19–20}. The temperature-

controlled stage of the microscope should be switched off in advance, i.e., before the rotor is added to the cells. For our setup, cooling of the stage takes about 10 min.

4.1. Prepare a general stock solution of the fluorescent molecular rotor BODIPY 2 (Stock 1, 25.7 mM).

4.1.1. Open BODIPY 2 in a sterile environment and weigh approximately 2 mg, using an accurate balance. Carefully place it in a microcentrifuge tube.

4.1.2. Use an automatic 20 μL pipette to add a 3 μL of a suitable solvent (e.g., DMSO).

4.1.3. Once the sample dissolves completely in DMSO, add 297 μL of sterile PBS and mix thoroughly using an automatic 200 μL pipette.

NOTE: Store the stock solution in the refrigerator at +4 $^{\circ}\text{C}$ in dark packaging. Once resuspended, it can be stored in the refrigerator for several months.

4.2. Prepare a Stock 2 (8.9 mM) by adding 25 μL of the general stock solution (Stock 1) to a microcentrifuge tube, followed by 48 μL of sterile PBS. Mix gently using an automatic 200 μL pipette.

NOTE: Use stock 2 to prepare the final staining stock, which is applied for cell staining since micromolar concentration is required.

4.3. Gently replace the culture media in the dish (from step 3.1) with ice-cold Hank's solution without $\text{Ca}^{2+}/\text{Mg}^{2+}$ and incubate cells at +4 $^{\circ}\text{C}$ for 3 min.

NOTE: The use of ice-cold solution and incubation at +4 $^{\circ}\text{C}$ slows down the internalization of the molecular rotor, and local staining of the membrane persists for 20–30 min.

4.4. Prepare the final staining solution containing 4.5 μM of BODIPY 2 by adding 1 μL of the Stock 2 to 999 μL ice-cold Hank's solution or PBS.

NOTE: The concentration of BODIPY 2 in the final staining solution can be increased to ~ 10 μM without any toxic effects on cells, which result in a more efficient staining and greater number of collected photons. At higher concentrations, overloading of FLIM detector may occur.

4.5. Aspirate out the Hank's solution from the cell culture dish and replace with ice-cold 4.5 μM solution of BODIPY 2. The cells are imaged in BODIPY 2 solution without washing.

5. FLIM of the fluorescent molecular rotor in cells

NOTE: Always perform FLIM of the fluorescent molecular rotor after FLIM of metabolic cofactors because fluorescence spectrum of BODIPY 2 is overlapped with the emission of endogenous cofactors NAD(P)H and FAD^{12,17,18}.

5.1. Transfer the dish with the stained cells to the microscope stage (~20 °C) for imaging.

5.2. Set the following parameters for one-photon mode in the laser scanning microscope's software: **Excitation** at the wavelength of 488 nm with an argon ion laser, **Laser power** 1%–2%, **Emission** at 500–550 nm wavelength.

5.3. Use an oil immersion objective lens C Plan-Apochromat 40x/1.3 NA for image acquisition.

5.4. Press the **Live** button. Start scanning and using the XY and Z positioning by an integrated motorized stage. Adjust the focus and obtain a transmission and fluorescence intensity images of cells in a preview window. **Save** the obtained images, if required.

5.5. Check on the overlapped transmission and fluorescence image to see whether the fluorescence of the rotor is coming from the expected location (plasma membrane of cell).

5.6. Enter the following parameters in the menu of SPCM software of FLIM module: **Collection time**: 60 s; **TAC Range**: 5.00E-8; **CFD Limit Low**: -29.41; **ADC Resolution**: 256, **Image Size**: 256 x 256 pixels.

NOTE: Depending on the system configuration and detectors used for FLIM, the parameters of image acquisition may vary.

5.7. Adjust the Ti:Sapphire laser of the microscope to a **wavelength** of 850 nm and the **Laser Power** to 1%–2% for two-photon FLIM.

5.8. Select the **Continuous** tab in the laser scanning microscope software, and then press **Start** in the SPCM software. Scan the sample for 60 s, stop scanning, and save the obtained FLIM image.

5.9. Check the obtained FLIM data. For this, load the raw data in the FLIM data analysis SPCImage software, select a pixel in the cell's membrane by placing the cursor over it and analyze the fluorescence decay in this pixel. Pixel intensities should be ≥5,000 per decay (possibly including binning) at a reasonable collection time (60–120 s).

5.10. Repeat steps 5.4–5.8 to record FLIM images of cells from different fields of view.

NOTE: FLIM measurements of live cells stained with BODIPY 2 should be limited to ~30 min after adding BODIPY 2.

6. Data analysis

6.1. Fluorescence intensity analysis: redox ratio

6.1.1. Open images of fluorescence intensity of NAD(P)H and FAD using ImageJ.

6.1.2. Highlight a cell-free area in the NAD(P)H image using a circle or a square option. Click on **Measure**, and then click on **Subtract** (select **Process** on the main panel, and then **Math** and **Subtract**) to subtract the obtained value of the background signal.

6.1.3. Repeat step 6.1.2 for FAD image.

6.1.4. Obtain the image of the redox ratio by dividing the FAD fluorescence intensity by NAD(P)H fluorescence intensity. Do this by selecting **Process** on the main panel, and then select **Image Calculator** and **Divide**; check the box **Create new window**, and then press **OK**.

6.1.5. Save the image in TIFF format.

6.1.6. To calculate the redox ratio, select the region of the cytoplasm in the specific cell on the TIFF image and press the **M** key. Repeat for all cells of interest.

6.1.7. Import the measurement to a spreadsheet document.

NOTE: Alternatively, fluorescence intensities of NAD(P)H and FAD in cells can be measured using standard software of the microscope and the redox ratio can be obtained by dividing these values in the spreadsheet software.

6.2. FLIM data analysis: metabolism

6.2.1. Import FLIM image of NAD(P)H into SPCImage software.

6.2.2. Apply a bi-exponential decay fit to the image by putting 2 in the **Components** section.

6.2.3. Fix the **Offset** parameter by checking the corresponding box in the SPCImage software.

6.2.4. Go to **Options** and select **Model**. Use **Incomplete Multiexponential** fitting model and **Fit Method MLE**.

6.2.5. Adjust binning to achieve pixel intensities of ≥ 5000 photons per decay curve.

6.2.6. Check χ^2 value. The $\chi^2 \leq 1.20$ indicates that the model used provides a reasonable fit.

6.2.7. Calculate the histogram of fluorescent lifetime in each image by clicking on the top menu **Calculate**, and then on **Decay Matrix**.

6.2.8. Select the area in the cytoplasm of the specific cell as a region of interest.

6.2.9. Analyze the short and long lifetime components (τ_1 and τ_2 , respectively) and the relative amplitudes of the lifetime components (a_1 and a_2 , where $a_1 + a_2 = 100\%$) by using the **Color** option.

6.2.10. Export the measurements to a spreadsheet software.

6.2.11. Repeat steps 6.2.8–6.2.10 for each cell of interest.

6.2.12. Repeat steps 6.2.1–6.2.11 for FAD image.

6.3. FLIM data analysis: viscosity

6.3.1. Import FLIM image into FLIM data analysis SPCImage software.

6.3.2. Remove the mark in the **Scatter** box.

6.3.3. Put 1 in the **Components** section, since the rotor fluorescence decay should fit to a monoexponential model.

6.3.4. Adjust binning to achieve a pixel intensity of ≥ 5000 photons per decay per pixel.

6.3.5. Check the χ^2 value in the plasma membrane. A value of $\chi^2 \leq 1.20$ indicates that the model used provides a reasonable fit. In the case of $\chi^2 \geq 1.20$, monoexponential approximation is not applicable, such data can indicate the dye aggregation and should be discarded. Aggregation makes it impossible to use the calibration curves and leads in incorrect viscosity estimates.

NOTE: Bi-exponential decays may be indicative of aggregation. On a microscope with FLIM module with variable filters, this can be detected by testing monomer and aggregate-specific emission wavelength ranges, 500–550 nm and 580–650 nm, as described in reference²¹.

6.3.6. Generate the histogram of the fluorescence lifetime τ for each image by clicking on the top menu **Calculate**, and then on **Decay Matrix**.

6.3.7. Select the region of plasma membrane of individual cell with monoexponential decay, $\chi^2 \leq 1.20$, using ROI option.

6.3.8. Export the value of fluorescence lifetime to a spreadsheet in Excel.

6.3.9. Repeat steps 6.3.7–6.3.8 for each cell of interest.

6.3.10. Convert experimentally measured lifetimes of BODIPY 2 (in ns) to viscosity values (in cP) using the following equation (previously obtained on the basis of the calibration plot of BODIPY in methanol/glycerol mixtures):

$$x = \frac{y^2}{0.0206}$$

where x — viscosity (in cP), y — fluorescence lifetime τ (in ns).

NOTE: IRF (Instrument Response Function) is an important part of FLIM fitting. In SPCImage IRF is automatically calculated from the rising edge of the fluorescence decay curves. Meanwhile, IRF can be recorded using non-fluorescent sample, e.g., ceramics, or a sample that produces SHG (Second Harmonic Generation) signal, e.g., collagen, urea crystals, or sugar. The use of the recorded IRFs is not recommended if there is an option to calculate it in the software.

REPRESENTATIVE RESULTS:

Using the protocol described here, we have visualized the metabolic co-factors and microscopic membrane viscosity in live cultured cells using FLIM. The measurements have been done in different cancer cell lines – human colorectal carcinoma HCT116, murine colon carcinoma CT26, human cervical cancer HeLa Kyoto, and human skin fibroblasts huFB.

Fluorescence intensity-based redox ratio FAD/NAD(P)H and fluorescence lifetimes of NAD(P)H and FAD allow assessing the cellular metabolic state (**Figure 1, Figure 2**). NAD(P)H and FAD localized mainly in the cytoplasm of the cells. Different cell types in our study displayed similar fluorescence lifetimes of NAD(P)H and flavins and contributions of the short- and long-lifetime fractions, which likely indicated that they had similar metabolic state in *in vitro* conditions. The fluorescence lifetimes and the relative contributions of the free (τ_1 , a_1) and protein-bound (τ_2 , a_2) NAD(P)H were measured to be ~0.54 ns, ~75% and ~2.5 ns, ~25%, respectively. For the quenched (τ_1 , a_1) and unquenched (τ_2 , a_2) FAD the fluorescence lifetimes and the relative contributions were ~0.35 ns, ~85% and ~2.0 ns, ~15%, respectively (**Table 1**).

Using the developed protocol, we investigated the metabolic response of HCT116 cells to chemotherapy with 5-fluorouracil. 5-fluorouracil was used at the dose of 4 μ M (the half maximal inhibitory concentration IC₅₀). The cells were incubated with the drug for 1 h or 24 h. Untreated cells served as a control. FLIM of NAD(P)H in the control and 5-fluorouracil-treated cells showed that the relative contribution of free NAD(P)H (a_1) decreased from $77.82 \pm 1.69\%$ to $66.34 \pm 1.71\%$ ($p = 0.0001$) in 24 h (**Figure 3**).

We have demonstrated the possibility of using the presented protocol for membrane viscosity measurements. BODIPY 2 effectively stained the plasma membrane of cancer cells (**Figure 4**). The cancer cell lines studied displayed different fluorescence lifetimes of the rotor, which means that they had different plasma membrane viscosity. The highest fluorescence lifetime of the rotor was registered in the membranes of HCT116 cells, 3.19 ± 0.14 ns, which corresponded to a viscosity value of 492 ± 33 cP. The membranes of CT26 cells were slightly less viscous - the fluorescence lifetime was 2.98 ± 0.16 ns, the viscosity was 432 ± 39 cP. The most fluid

membranes in this series were possessed by HeLa Kyoto cells - 2.65 ± 0.15 ns, which corresponded to 344 ± 36 cP.

Assessment of membrane viscosity in human skin fibroblasts was problematic, first, because BODIPY 2 entered the cells and diffusely spread throughout the cell very quickly, and second, because its fluorescence in the membrane of fibroblasts had bi-exponential decay (**Figure 4E**).

Clear staining of plasma membrane of all cancer cells studied is observed in the time-period from 5 to 30 min after adding BODIPY 2 to cells (**Figure 5**). Within this time, the fluorescence decay of BODIPY 2 fits to a monoexponential model. Further incubation with BODIPY 2 leads to the internalization of the dye and staining of the cell cytoplasm along with the plasma membrane. Analysis of the decay curves of BODIPY 2 located in the cytoplasm showed bi-exponential decays, presumably due to the presence of BODIPY 2 aggregates.

In parallel with metabolic assessments, we studied whether 5-fluorouracil induced changes to the plasma membrane viscosity in HCT116 cells (**Figure 6**). It is important to mention that the membrane viscosity was measured only in viable cells, since in rounded up cells with abnormal morphology (presumably, dead cells) the rotor did not stain the plasma membranes, but accumulated inside the cells, where its fluorescence decayed bi-exponentially, indicative of rotor aggregation²². The fluorescence lifetime of BODIPY 2 before the addition of 5-fluorouracil was 3.27 ± 0.14 ns, which corresponds to a viscosity value of 511 ± 43 cP. After 1 h incubation with 5-fluorouracil the fluorescence lifetime increased to 3.75 ± 0.24 ns, and the viscosity of the membranes was 697 ± 80 cP ($p < 0.0001$). After 24-h incubation with the drug, the fluorescence lifetime returned to a control level 3.18 ± 0.23 ns, and the viscosity was 516 ± 68 cP. It could be seen from the images that the number of cells in the field of view decreased significantly after the treatment. This is due to the detachment of altered cells in the course of the staining procedure.

FIGURE AND TABLE LEGENDS:

Figure 1: Metabolic imaging of HeLa cells using FLIM. (A) Bright-field microscopy, two-photon excited fluorescence intensity images of NAD(P)H and FAD, and the redox ratio FAD/NAD(P)H. (B) Two-photon FLIM of NAD(P)H. a_1 is the relative contribution of free NAD(P)H. Enlarged area is shown by the yellow-dashed square. On the enlarged image, the dashed red line indicates the area in the cytoplasm selected for analysis. (C) Two-photon FLIM of FAD. a_2 is the relative contribution of unquenched FAD. (D) Typical fluorescence decay curve of NAD(P)H obtained in SPCImage software: the experimental data (blue dots), bi-exponential fit (red curve), instrument response function (green curve). Bar is 50 μ m, applicable to all images. (E) Representative distributions of the fluorescence lifetime parameters (τ_1 , τ_2 , a_1 , a_2 , χ^2) in HeLa cells.

Figure 2: FLIM of NAD(P)H in HCT116, CT26, and huFB cells. Bar is 50 μ m, applicable to all images. The color-coded images show the relative contribution of free NAD(P)H (a_1 , %).

Table 1: Fluorescence lifetime parameters of NAD(P)H and FAD in various cell lines. Mean \pm

SD, n = 25–50 cells.

Figure 3: FLIM of NAD(P)H in HCT116 cells after chemotherapy. (A) The relative contribution of free NADH (a_1 , %) before (control) and in 24 h after chemotherapy with 5-fluorouracil. Bar is 50 μ m. (B) Quantification of a_1 NAD(P)H in control and treated cells. Mean \pm SD, n = 25–50 cells.

Figure 4: Mapping of plasma membrane viscosity of cultured cancer cells using fluorescent molecular rotor BODIPY 2 and FLIM. (A) Bright-field microscopy, one-photon excited fluorescence intensity image of BODIPY 2, two-photon excited FLIM, and the distribution of the χ^2 value. (B) FLIM images of CT26, HeLa and huFB cells stained with BODIPY 2. The color-coded images show the fluorescence lifetime of BODIPY 2 (τ , ns). Bar is 40 μ m, applicable to all images. (C) Quantification of plasma membrane microviscosity in the cancer cells. Mean \pm SD, 30–50 cells. (D) Typical fluorescence decay curve of BODIPY 2 obtained from HCT116 cancer cells in SPCImage software: the experimental data (blue dots), bi-exponential fit (red curve), instrument response function (green curve). (E) Fluorescence decay curve of BODIPY 2 obtained from the fibroblasts huFb. This fit is unacceptable due to poor χ^2 .

Figure 5: Monitoring fluorescence lifetime of molecular rotor BODIPY 2 in HeLa cells. (A) FLIM of the cells at the indicated time-points after adding BODIPY 2. (B) Enlarged area shown by the yellow-dashed square in A (5 min). The dashed red line indicates the area in the plasma membrane selected for analysis. (C) Distribution of the χ^2 value after 5 min and 60 min of incubation with BODIPY 2. BODIPY 2 located in the plasma membrane shows monoexponential decay with the $\chi^2 \leq 1.2$. BODIPY 2 located in the cytoplasm has poor χ^2 with monoexponential fitting.

Figure 6. Mapping of plasma membrane viscosity in untreated HCT116 cells and cells after 1- and 24-hours exposure to 5-fluorouracil. (A) Representative fluorescence lifetime images of the control and treated HCT116 cells (B) Quantification of plasma membrane microviscosity in the cells. Mean \pm SD, 20–30 cells.

DISCUSSION:

This protocol illustrates the possibilities of FLIM for multiparametric, functional, and biophysical analysis of cancer cells. The combination of the optical metabolic imaging based on endogenous fluorescence and the measurements of plasma membrane viscosity using exogenous labeling with fluorescent molecular rotor enables us to characterize the interconnections between these two parameters in live cancer cells in a cell culture and follow the changes in response to chemotherapy.

Two-photon excited fluorescence lifetime imaging microscopy (FLIM) is a promising technique for a non-invasive, sensitive, quantitative, high-resolution assessment of a functional state of living cells and tissues. Fluorescent chemical and genetically encoded sensors based on lifetime detection are currently available to visualize various physiological and physical-chemical parameters, including ion concentrations, pH, enzyme activity, hypoxia, cell cycle, viscosity, membrane potential, and others. In addition, FLIM can capture metabolic features of cells using

intrinsic fluorescence from NAD(P)H and flavin co-factors. Unlike the fluorescence intensity, fluorescence lifetime allows to overcome difficulties associated with an unknown and/or unstable fluorophore concentration, photobleaching, instrument configurations (e.g., excitation intensity, nonuniform illumination, and optical path length), absorption and scattering events²³. With an ability to measure multiple parameters from a single sample, FLIM becomes an increasingly popular modality in biomedical applications.

Depending on the microscope and the laser, different objectives and laser powers can be used. For two-photon excitation, oil- or water-immersion objectives with a high numerical aperture (>1) are preferred. The laser power is selected based on the available objective and should be adjusted to avoid photobleaching and saturation issues. Multiphoton microscopy is normally performed at laser power below 10 mW, which is considered to be safe for live cells. Image size is selected based on personal preferences.

One of the most useful aspects of the FLIM technique is the ability to noninvasively examine metabolic processes on a label-free basis, relying on endogenous fluorescence from coenzymes, NAD(P)H and FAD/FMN. The ability to probe metabolism on a single-cell level, dynamically over time, in live cells using entirely endogenous sources of contrast offers significant advantages over conventional metabolic assays, such as detection of metabolites (e.g., glucose, glutamine, lactate, ATP) or activity of metabolism-related genes or enzymes. Metabolic FLIM has proven to be a highly sensitive approach to differentiate cancerous and normal cells^{24–27} and detect the responses to anti-cancer therapies *in vitro* and *in vivo*^{28–31}. Previously, this methodology has been used in our lab to analyze metabolic state of cancer cells undergoing apoptosis³², to follow the metabolic response to chemotherapeutic agents^{30,33–34}, and metabolic shifts accompanying cancer cells-fibroblasts interactions³⁵.

Fluorescence decays of NAD(P)H and flavins are commonly described by a bi-exponential function. For adequate bi-exponential fitting, pixel intensities should be $\geq 5,000$ photons per decay curve, possibly with binning. On the system used, 5,000 photons per decay curve (binning 1) are typically collected at the photon counting rate $1\text{--}2 \times 10^5$ photons/s.

In the present work, we obtained the optical metabolic metrics for different cancer cell lines and human skin fibroblasts. All the measured fluorescence lifetimes of NAD(P)H and flavins correlate with those reported in the literature^{36–37}. Due to specifics of metabolism, fluorescence intensity of flavins in cancer cell lines is typically lower than in normal cells (e.g., fibroblasts or mesenchymal stem cells). Therefore, the analysis of fluorescence lifetime in cancer cells requires applying the pixel binning to adjust the number of photons to $\geq 5,000$. Notably, the binning option is used if increase of the laser power or image collection time is impossible due to morphological alterations (an indicator of a cell damage) or photobleaching. In the present protocol, a binning factor of 3–4 is used for flavins in cancer cells and 2–3 in fibroblasts. A binning factor 1–2 is used for NAD(P)H in cells at the indicated settings. Keep in mind that large binning decreases image resolution.

Each of the values extracted from the bi-exponential decay (τ_1 , a_1 , τ_2 , a_2) contains information about different parameters of the molecular environment. Specifically, long lifetime component τ_2 depends on the set of NAD(P)H-binding proteins in the case of NAD(P)H and contribution of FMN in the case of flavins. The amplitudes a_1 and a_2 reflect the relative amounts of two fractions of the fluorophores – free and bound NAD(P)H, quenched and unquenched flavins. Among others, a_1 and a_2 values are the most variable metrics upon metabolic perturbations³⁸. If τ_1 and/or τ_2 values vary for some reasons, mean fluorescence lifetime ($\tau_m = (a_1 \cdot \tau_1 + a_2 \cdot \tau_2) / (a_1 + a_2)$) can also be a relevant metric. Taking into account that fluorescence of flavins in cancer cells is typically weak, the relative contributions of free and bound NAD(P)H (a_1 , a_2 or their ratio a_1/a_2) are most frequently used as a biomarker of metabolic changes.

Interpretation of the NAD(P)H FLIM data from the biochemical standpoint of view is rather easy, since NADH is primarily involved in energy metabolism. The only fluorophore that can complicate the analysis of the data is protein-bound phosphorylated form of NADH, NADPH (τ 4.4 ns)³⁹. However, it is present in cancer cells in lower concentration compared with NADH⁴⁰. Fluorescence lifetimes of flavin cofactors are more difficult to interpret, since they participate in a number of processes, besides energy production, and contribution of FMN (τ ~4.7 ns) can be essential.

In the present protocol, we use the weighted least-square method of the fluorescence decay fitting as a gold standard. Meanwhile, non-fitting, that is non-parametric, approaches to FLIM data analysis are increasingly developed^{41–44}.

In addition to fluorescence lifetime measurements, our protocol provides methodology for the assessment of the optical redox ratio using laser scanning microscopy. The optical redox ratio, first introduced by Britton Chance, as a ratio of fluorescence intensities of the reduced and oxidized cofactors, represents a simple metric of the cellular redox status. Different equations can be used to calculate the optical redox ratio, e.g., NAD(P)H/FAD^{29,31} or FAD/(FAD+NAD(P)H)^{38,45}. The choice of the equation depends on the task and characteristics of the signal. It was reported that the optical redox ratio correlates well with the biochemical redox ratio of $NAD^+/(NADH+NAD^+)$ ⁴⁵ and the oxygen consumption rate⁴⁶. However, interpretation of the optical redox ratio is not always straightforward because fluorescence intensity is affected by many factors besides concentration of the fluorophores (see above). Therefore, more attention should be paid to the photobleaching effects in the imaged cells in the course of data acquisition. Since excitation power affects the emission intensity, laser power at the specific wavelength (750 nm or 900 nm) should be the same for all collected images for redox ratio measurements.

We used metabolic FLIM for the study of metabolic alterations in human colorectal cancer cells HCT116 induced by 5-fluorouracil, a standard chemotherapeutic drug of antimetabolite class (pyrimidine analog). Treatment with 5-fluorouracil resulted in an increase of the bound NAD(P)H fraction after 24 h, whereas no metabolic changes were observed after 1 h incubation (data not shown). In our earlier studies on cell cultures and mouse tumor models, we showed that similar changes in NAD(P)H fluorescence lifetime developed in response to the drugs

657 having different mechanisms of action, e.g. cisplatin, paclitaxel, irinotecan, and associated this
658 with inhibition of the cell proliferation^{30,33}. We speculate that the observed changes in NAD(P)H
659 fluorescence could be caused by a shift in energy metabolism to a more oxidative level due to
660 activation of OXPHOS and/or decrease in the rate of glycolysis. Although the FLIM alone does
661 not allow to specify exactly the changes in metabolic pathways, it identifies the intrinsic
662 biomarkers of cellular response to the therapy.

663
664 While we used this protocol to visualize the metabolic changes only in the selected time-points
665 (0, 1, and 24 h), it can in principle be used for dynamic live-cell imaging. In the prolonged
666 experiments intended for repeated imaging of the same cells, the optimal balance between the
667 amount of acquired data and the potential of cells damage and photobleaching caused by
668 excessive laser exposure needs to be considered.

669
670 In the current protocol, imaging of metabolism and viscosity was performed sequentially
671 (metabolism was imaged first) because fluorescence of viscosity probe BODIPY 2 is overlapped
672 with NAD(P)H (slightly) and flavins (significantly). In the case of NAD(P)H, this issue can be
673 solved by using very narrow filters for a more accurate separation of the signals. In the case of
674 FAD, this is problematic, because its emission spectrum closely matches the emission spectrum
675 of BODIPY 2. Since the molecular rotor enters into the cell very quickly, while preserving
676 sufficient concentration in the plasma membrane, its fluorescence in the cytoplasm will distort
677 fluorescence decays of metabolic cofactors. Simultaneous imaging of the two parameters could
678 be possible with the use of red-emitting viscosity probes. Several red fluorescent viscosity
679 probes have been developed recently and used to monitor the mitochondrial and lysosomal
680 viscosity in living cells^{47–50}.

681
682 Since the rotor BODIPY 2 is an exogenous dye that is retained in plasma membrane only within
683 ~30 min, long-term monitoring of viscosity in the same cells is not possible with this technique,
684 and separate culture dishes have to be prepared for different time-points of experiment. At
685 longer incubation times (>30 min), endocytosis of BODIPY 2 and its aggregation inside cells may
686 occur, which can distort fluorescence decays recorded from the plasma membrane, as some
687 volume of the cytoplasm is unavoidably captured upon FLIM data processing (via binning). In
688 addition, the concentration of rotor in the plasma membrane decreases after ~30–60 min,
689 which results in a lower photon count rate.

690
691 As shown in this study, plasma membrane viscosity of cancer cells lays in the range ~340–490
692 cP and differs for different cancer cells lines. In fibroblasts, we failed to measure viscosity of
693 membrane because the rotor BODIPY 2 showed bi-exponential fluorescence decay in the
694 membrane and internalized into the cells very quickly. We assume that this is associated with
695 specific biophysical properties of the fibroblasts plasma membrane. The membrane of normal
696 fibroblasts is shown to be more fluid (less viscous) than the membrane of cancer cells⁵¹. It is
697 known that increased fluidity of plasma membrane promotes cell motility, inherent in the cells
698 of mesenchymal phenotype, such as fibroblasts.

Upon 1 h exposure to 5-fluorouracil, we observed a statistically significant increase in the viscosity of the plasma membrane of cultured HCT116 cancer cells. Unlike 5-fluorouracil, cisplatin caused a non-significant decrease of membrane viscosity of cancer cells at this time-point²², which indicated that the type and dynamics of the changes were drug-specific.

Overall, these results show that microviscosity of plasma membrane does not directly correlate with the metabolic activity of cells. In conclusion, please note that while we used Carl Zeiss LSM 880 microscope and Becker&Hickl FLIM module, with the appropriate settings, other confocal microscopy and/or FLIM systems can be successfully used as well. With the advancement of the methods of FLIM data analysis, automatic image segmentation and processing will be possible. The protocols demonstrated here for FLIM of metabolism and microviscosity in cultured cancer cells can be used independently and easily applied to other cell types and different interventions.

ACKNOWLEDGMENTS:

The development of protocol of metabolic imaging was supported by the Ministry of Health of the Russian Federation (Government Assignment, registration No. AAAA-A20-120022590098-0). The study of viscosity was supported by the Russian Science Foundation (Project No. 20-14-00111). The authors are thankful to Anton Plekhanov (PRMU) for his help with video production.

DISCLOSURES:

The authors have nothing to disclose.

REFERENCES:

1. Vazquez, A. et al. Cancer metabolism at a glance. *Journal of Cell Science*. **129** (18), 3367–3373 (2016).
2. Li, Z., Zhang, H. Reprogramming of glucose, fatty acid, and amino acid metabolism for cancer progression. *Cellular and Molecular Life Sciences*. **73** (2), 377–392 (2015).
3. Strickaert, A. et al. Cancer heterogeneity is not compatible with one unique cancer cell metabolic map. *Oncogene*. **36** (19), 2637–2642 (2016).
4. Szlasa, W., Zendran, I., Zalesińska, A., Tarek, M., Kulbacka, J. Lipid composition of the cancer cell membrane. *Journal of Bioenergetics and Biomembranes*. **52**, 321–342 (2020).
5. Preta, G. New insights into targeting membrane lipids for cancer therapy. *Frontiers in Cell and Developmental Biology*. **8**, 571237 (2020).
6. Kojima, K. Molecular aspects of the plasma membrane in tumor cells. *Nagoya Journal of Medical Science*. **56**, 1–18 (1993).
7. Datta, R., Heaster, T. M., Sharick, J. T., Gillette, A. A., Skala, M. C. Fluorescence lifetime imaging microscopy: fundamentals and advances in instrumentation, analysis, and applications. *Journal of Biomedical Optics*. **25** (7), 071203 (2020).
8. Becker, W. Advanced time-correlated single photon counting applications. *Springer Series in Chemical Physics* (2015).

9. Shirmanova, M. V., Shcheslavskiy, V. I., Lukina, M. M., Becker, W., Zagaynova, E. V. Exploring tumor metabolism with time-resolved fluorescence methods: From single cells to a whole tumor. *Multimodal Optical Diagnostics of Cancer*. **3**, 133–155 (2020).
10. Kalinina, S., Rück, A. FLIM and PLIM in biomedical research. An innovative way to combine autofluorescence and oxygen measurements. *Photonics & Lasers in Medicine*. **5** (4), 257–266 (2016).
11. Kuimova, M. K. Molecular rotors image intracellular viscosity. *Chimia*. **66** (4), 159–165 (2012).
12. Kuimova, M. K. Mapping viscosity in cells using molecular rotors. *Physical Chemistry Chemical Physics*. **14** (37), 12671 (2012).
13. Haidekker, M. A., Theodorakis, E. A. Molecular rotors—fluorescent biosensors for viscosity and flow. *Organic & Biomolecular Chemistry*. **5**, 1669–1678 (2007).
14. Liu, X. et al. Molecular mechanism of viscosity sensitivity in BODIPY rotors and application to motion-based fluorescent sensors. *ACS Sensors*. **5** (3), 731–739 (2020).
15. Shirmanova, M. V., Shimolina, L. E., Lukina, M. M., Zagaynova, E. V., Kuimova, M. K. Live cell imaging of viscosity in 3D tumour cell models. In: Dmitriev R. (eds) *Multi-Parametric Live Cell Microscopy of 3D Tissue Models. Advances in Experimental Medicine and Biology*. **1035**, 143–153 (2017).
16. Shimolina, L. E. et al. Imaging tumor microscopic viscosity in vivo using molecular rotors, *Scientific Reports*. **7**, 41097 (2017).
17. Scott, T. G., Spencer, R. D., Leonard, N. J., Weber, G. Synthetic spectroscopic models related to coenzymes and base pairs. V. Emission properties of NADH. Studies of fluorescence lifetimes and quantum efficiencies of NADH, AcPyADH, [reduced acetylpyridineadenine dinucleotide] and simplified synthetic models. *Journal of the American Chemical Society*. **92** (3), 687–695 (1970).
18. Harvey, R. A., Damle, S. A fluorescent modification of flavin adenine dinucleotide. *FEBS Letters*. **26** (1–2), 341–343 (1972).
19. Kubánková, M., Summers, P., López-Duarte, I., Kiryushko, D. Kuimova, M. K. Microscopic viscosity of neuronal plasma membranes measured using fluorescent molecular rotors: Effects of oxidative stress and neuroprotection. *ACS Applied Materials and Interfaces*. **11**, 36307–36315 (2019).
20. Kubánková, M., López-Duarte, I., Kiryushko, D. Kuimova, M. K. Molecular rotors report on changes in live cell plasma membrane microviscosity upon interaction with beta-amyloid aggregates. *Soft Matter*. **14**, 9466–9474 (2018).
21. Wu, Y. et al. Molecular rheometry: Direct determination of viscosity in Lo and Ld lipid phases via fluorescence lifetime imaging. *Physical Chemistry Chemical Physics*. **15** (36), 14986 (2013).
22. Shimolina, L. E. et al. Mapping cisplatin-induced viscosity alterations in cancer cells using molecular rotor and fluorescence lifetime imaging microscopy. *Journal of Biomedical Optics*. **25** (12), 126004 (2020).
23. Berezin, M. Y., Achilefu, S., Fluorescence lifetime measurements and biological imaging, *Chemical Reviews*. **110** (5), 2641–2684 (2010).

24. Skala, M. C. et al. In vivo multiphoton fluorescence lifetime imaging of protein-bound and free nicotinamide adenine dinucleotide in normal and precancerous epithelia. *Journal of Biomedical Optics*. **12** (2), 024014 (2007).
25. Rück, A., Hauser, C., Mosch, S., Kalinina, S. Spectrally resolved fluorescence lifetime imaging to investigate cell metabolism in malignant and nonmalignant oral mucosa cells. *Journal of Biomedical Optics*. **19** (9), 096005 (2014).
26. Lee, D.-H., Li, X., Ma, N., Digman, M. A., Lee, A. P. Rapid and label-free identification of single leukemia cells from blood in a high-density microfluidic trapping array by fluorescence lifetime imaging microscopy. *Lab on a Chip*. **18** (9), 1349–1358 (2018).
27. Lukina, M. M. et al. Interrogation of tumor metabolism in tissue samples ex vivo using fluorescence lifetime imaging of NAD(P)H. *Methods and Applications in Fluorescence*. **8** (1), 014002 (2019).
28. Alam, S. R. et al. Investigation of mitochondrial metabolic response to doxorubicin in prostate cancer cells: An NADH, FAD and Tryptophan FLIM assay. *Scientific Reports*. **7** (1), 10451 (2017).
29. Walsh, A. J. et al. Quantitative optical imaging of primary tumor organoid metabolism predicts drug response in breast cancer. *Cancer Research*. **74** (18), 5184–5194 (2014).
30. Lukina, M. M. et al. In vivo metabolic and SHG imaging for monitoring of tumor response to chemotherapy. *Cytometry Part A*. **95** (1), 47–55 (2019).
31. Shah, A. T. et al. Optical metabolic imaging of treatment response in human head and neck squamous cell carcinoma. *PLoS One*. **9** (3), e90746 (2014).
32. Sergeeva, T. F. et al. Relationship between intracellular pH, metabolic co-factors, and caspase-3 activation in cancer cells during apoptosis. *Biochimica et Biophysica Acta (BBA) - Molecular Cell Research*. **1864** (3), 604–611 (2017).
33. Shirmanova, M. V. et al. Chemotherapy with cisplatin: insights into intracellular pH and metabolic landscape of cancer cells in vitro and in vivo. *Scientific Reports*. **7**, 8911 (2017).
34. Lukina, M. M. et al. Metabolic cofactors NAD(P)H and FAD as potential indicators of cancer cell response to chemotherapy with paclitaxel. *Biochimica et Biophysica Acta (BBA) - General Subjects*. **1862** (8), 1693–1700 (2018).
35. Druzhkova, I. N. et al. The metabolic interaction of cancer cells and fibroblasts – coupling between NAD(P)H and FAD, intracellular pH and hydrogen peroxide. *Cell Cycle*. **15** (9), 1257–1266 (2016).
36. Lakowicz, J., Szmacinski, H., Nowaczyk, K., Johnson, M. Fluorescence lifetime imaging of free and protein bound NADH. *Proceedings of the National Academy of Sciences of the United States of America*. **89** (4), 1271–1275 (1992).
37. Van den Berg, P. A. W., Feenstra, K. A., Mark, A. E., Berendsen, H. J. C., Visser, A. J. W. G. Dynamic conformations of flavin adenine dinucleotide: Simulated molecular dynamics of the flavin cofactor related to the time-resolved fluorescence characteristics. *The Journal of Physical Chemistry B*. **106** (34), 8858–8869 (2002).
38. Liu, Z. et al. Mapping metabolic changes by noninvasive, multiparametric, high-resolution imaging using endogenous contrast. *Science Advances*. **4** (3), eaap9302 (2018).
39. Blacker, T. S. et al. Separating NADH and NADPH fluorescence in live cells and tissues using FLIM. *Nature Communications*. **5**, 3936 (2014).

827 40. Lu, W., Wang, L., Chen, L., Hui, S., Rabinowitz, J. D. Extraction and quantitation of
828 nicotinamide adenine dinucleotide redox cofactors. *Antioxidants and Redox Signaling*. **28** (3),
829 167–179 (2018).

830 41. Ranjit, S., Malacrida, L., Jameson, D. M., Gratton, E. Fit-free analysis of fluorescence lifetime
831 imaging data using the phasor approach. *Nature Protocols*. **13** (9), 1979–2004 (2018).

832 42. Stringari, C. et al. Phasor approach to fluorescence lifetime microscopy distinguishes
833 different metabolic states of germ cells in a live tissue. *Proceedings of the National Academy of
834 Sciences of the United States of America*. **108** (33), 13582–13587 (2011).

835 43. Smith, J. T. et al. Fast fit-free analysis of fluorescence lifetime imaging via deep learning.
836 *Proceedings of the National Academy of Sciences of the United States of America*. **116** (48),
837 24019–24030 (2019).

838 44. Wang, S., Chacko, J. V., Sagar, A. K., Eliceiri, K. W., Yuan M. Nonparametric empirical
839 Bayesian framework for fluorescence-lifetime imaging microscopy. *Biomedical Optics Express*.
840 **10** (11), 5497–5517 (2019).

841 45. Quinn, K. P. et al. Quantitative metabolic imaging using endogenous fluorescence to detect
842 stem cell differentiation. *Scientific Reports*. **3** (1), 3432 (2013).

843 46. Hou, J. et al. Correlating two-photon excited fluorescence imaging of breast cancer cellular
844 redox state with seahorse flux analysis of normalized cellular oxygen consumption. *Journal of
845 Biomedical Optics*. **21** (6), 060503 (2016).

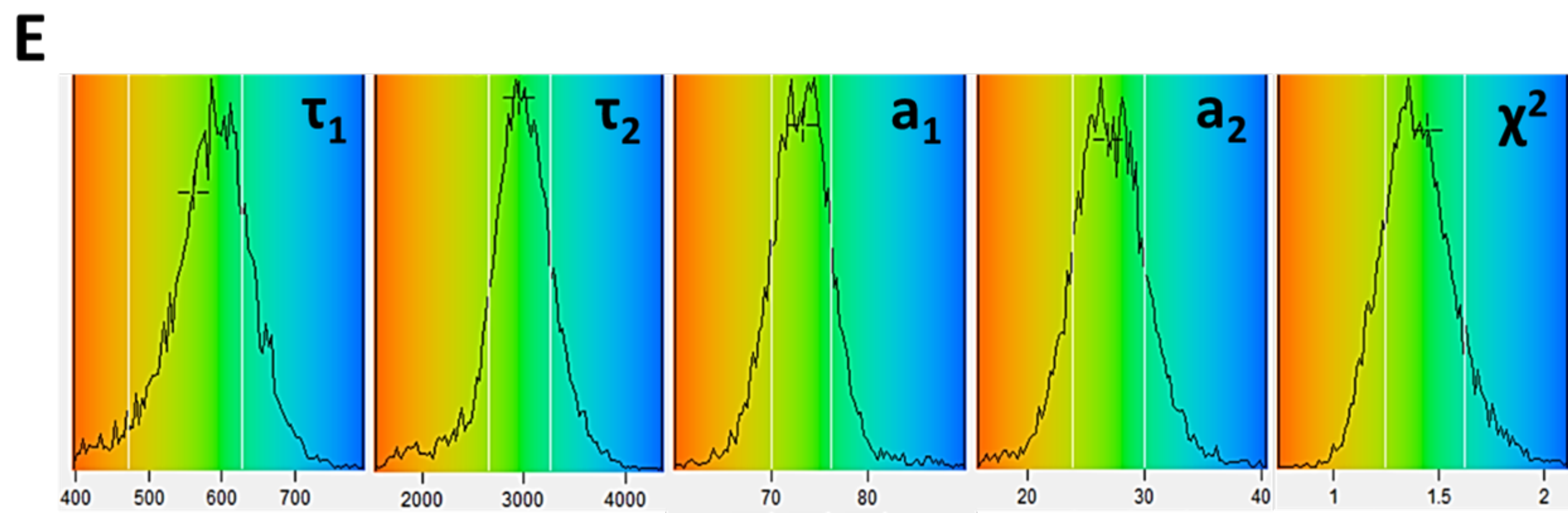
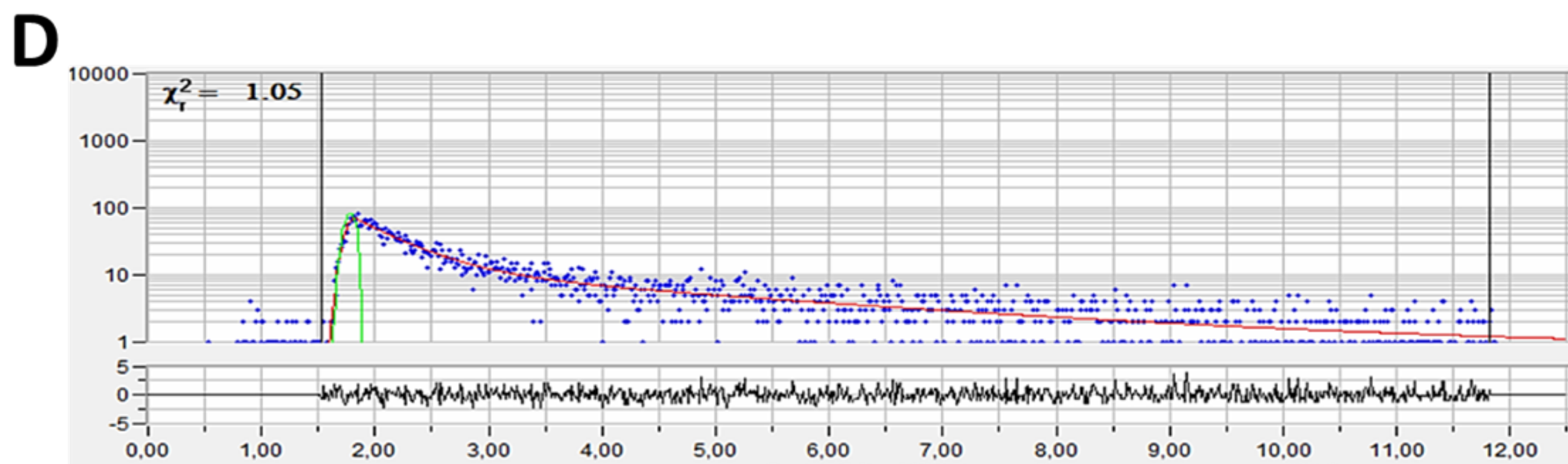
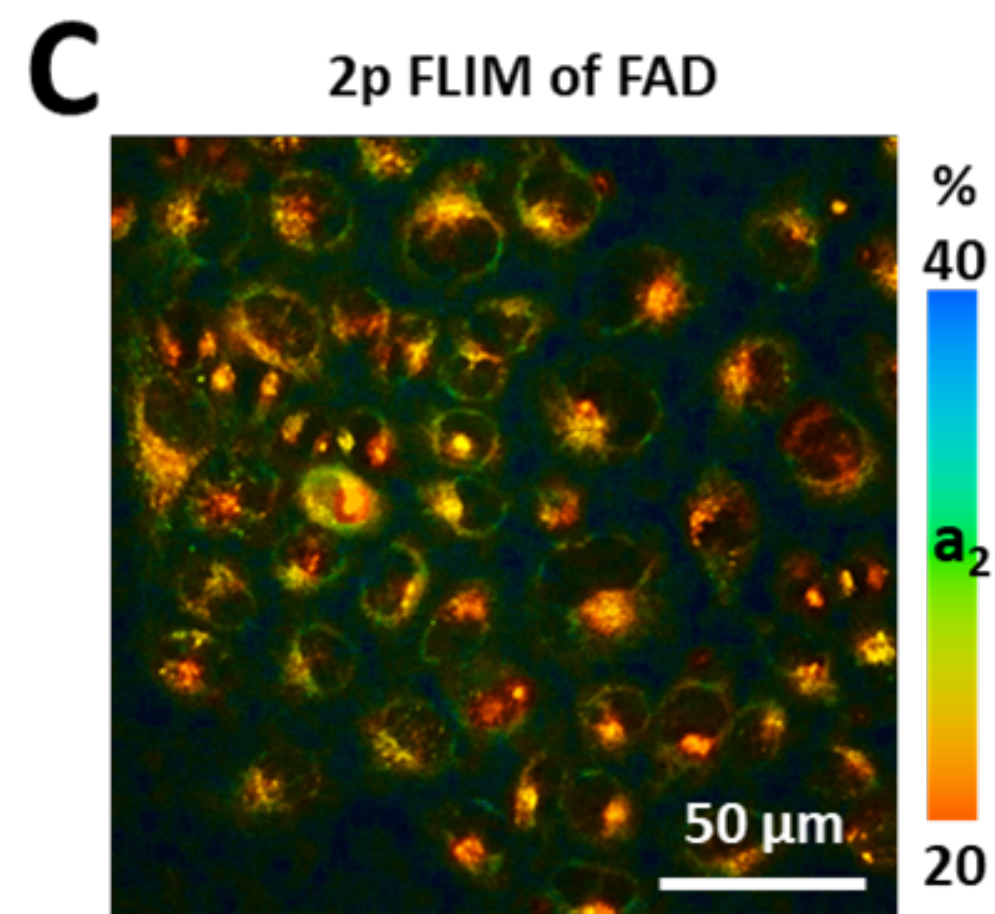
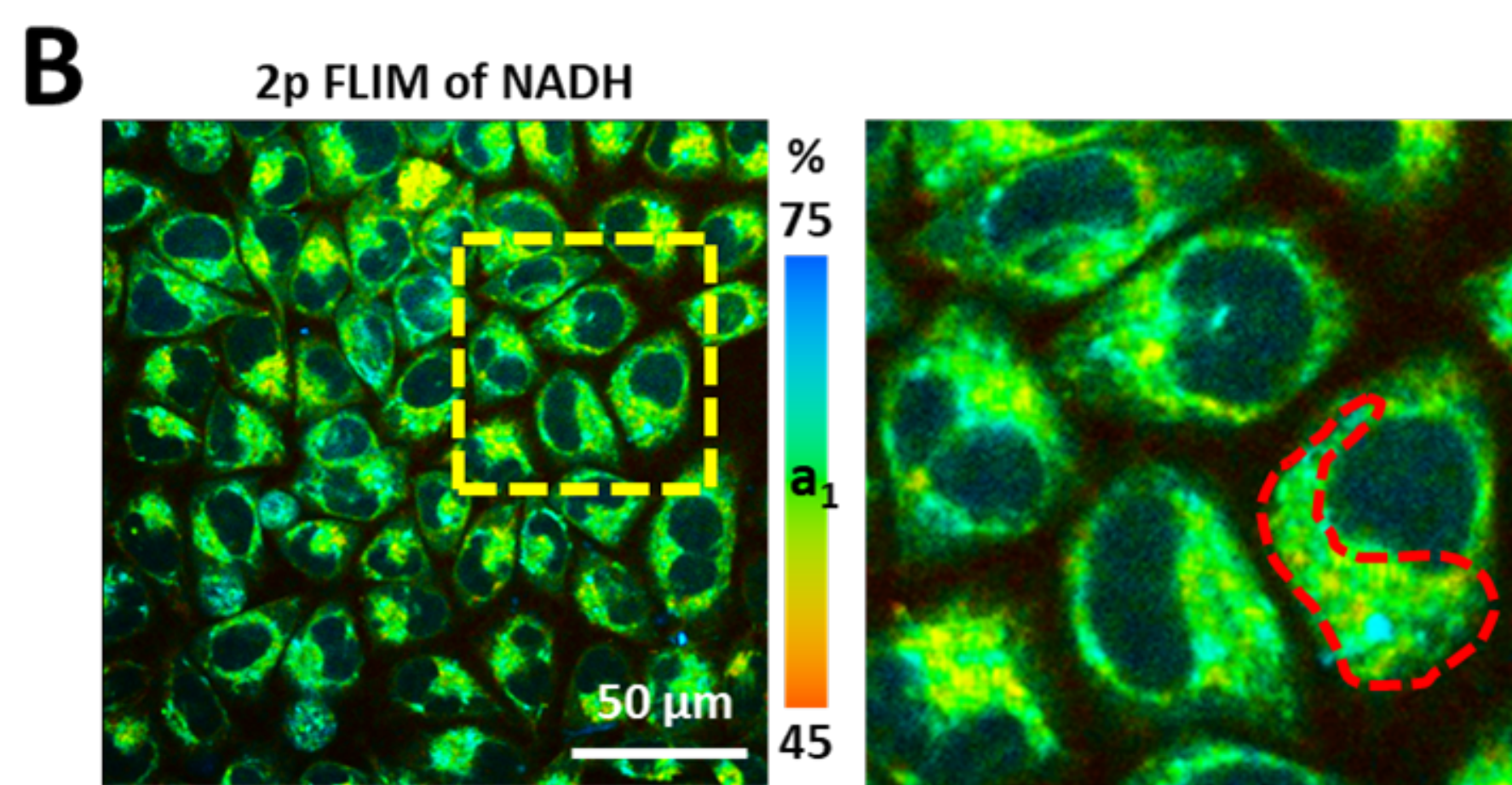
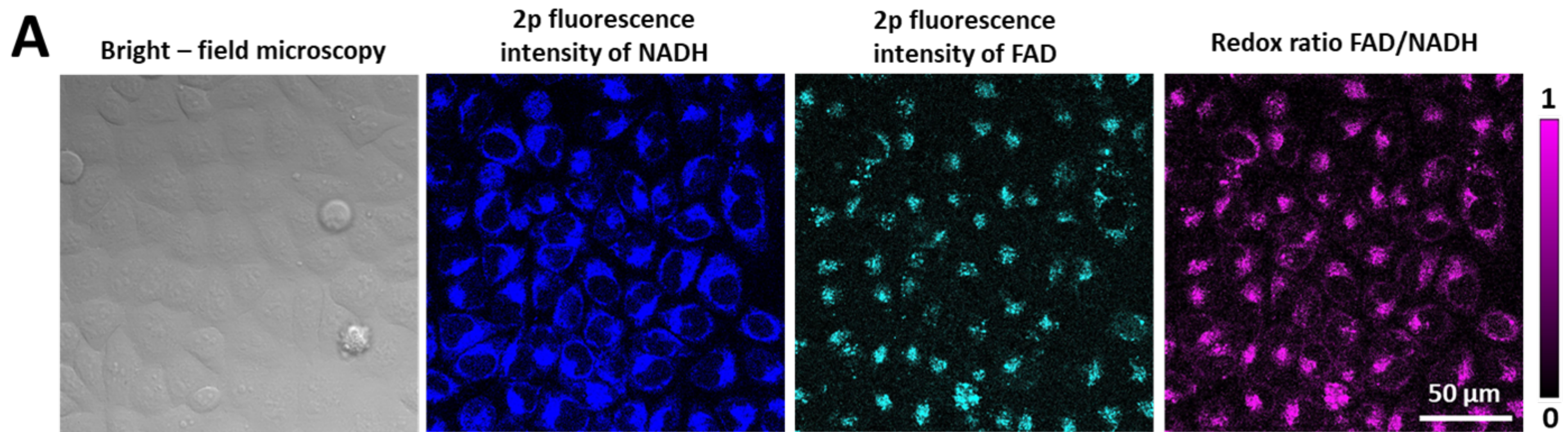
846 47. Wang, H. et al. Red-emitting fluorescence probe for sensing viscosity in living cells. *Chemical
847 Papers*. **74**, 1071–1078 (2020).

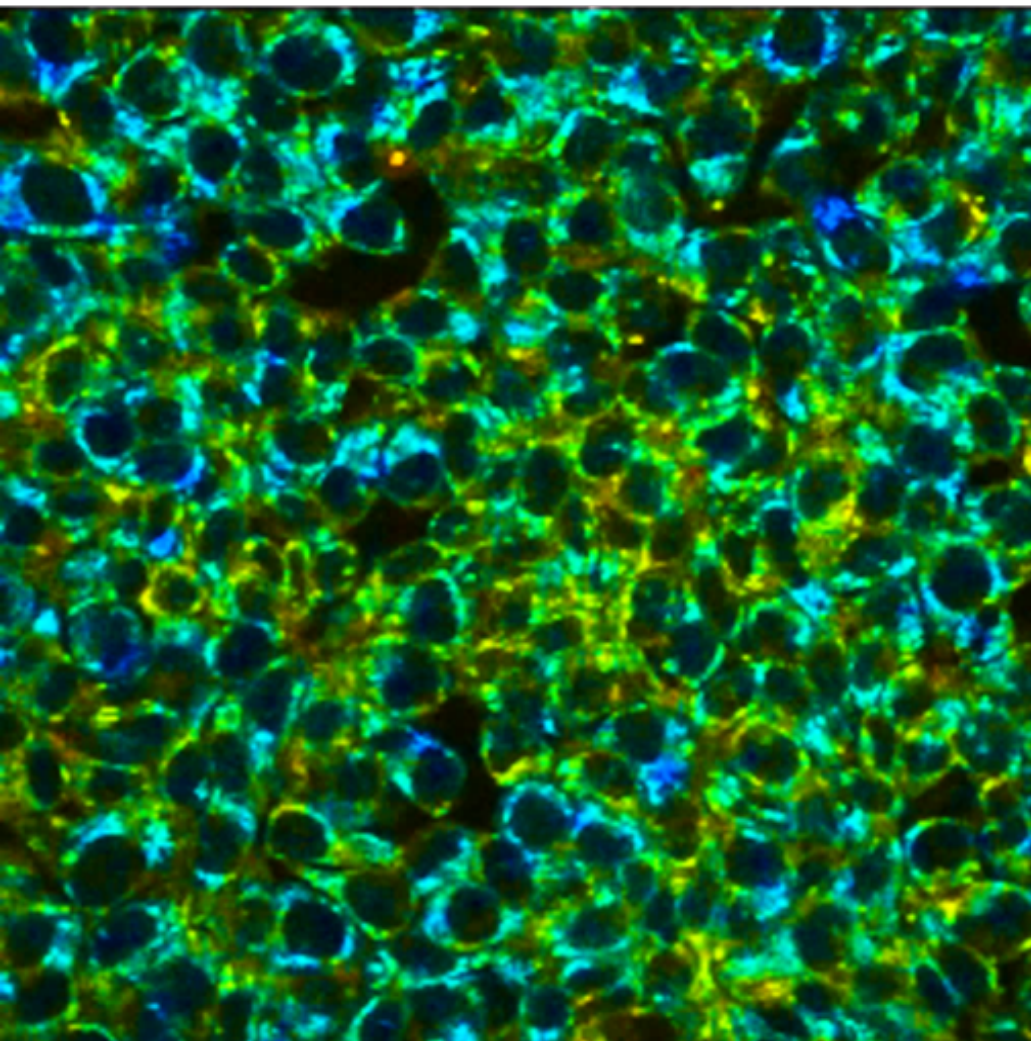
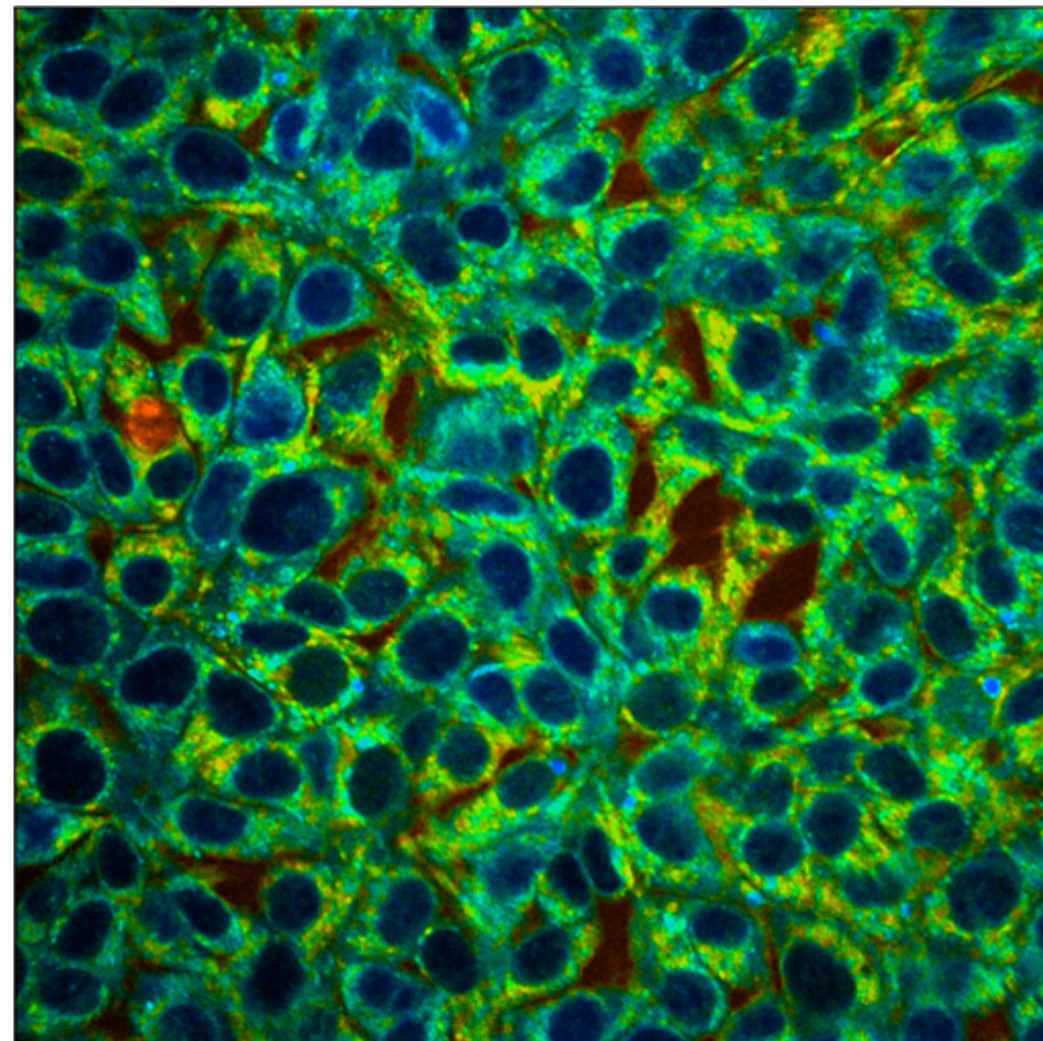
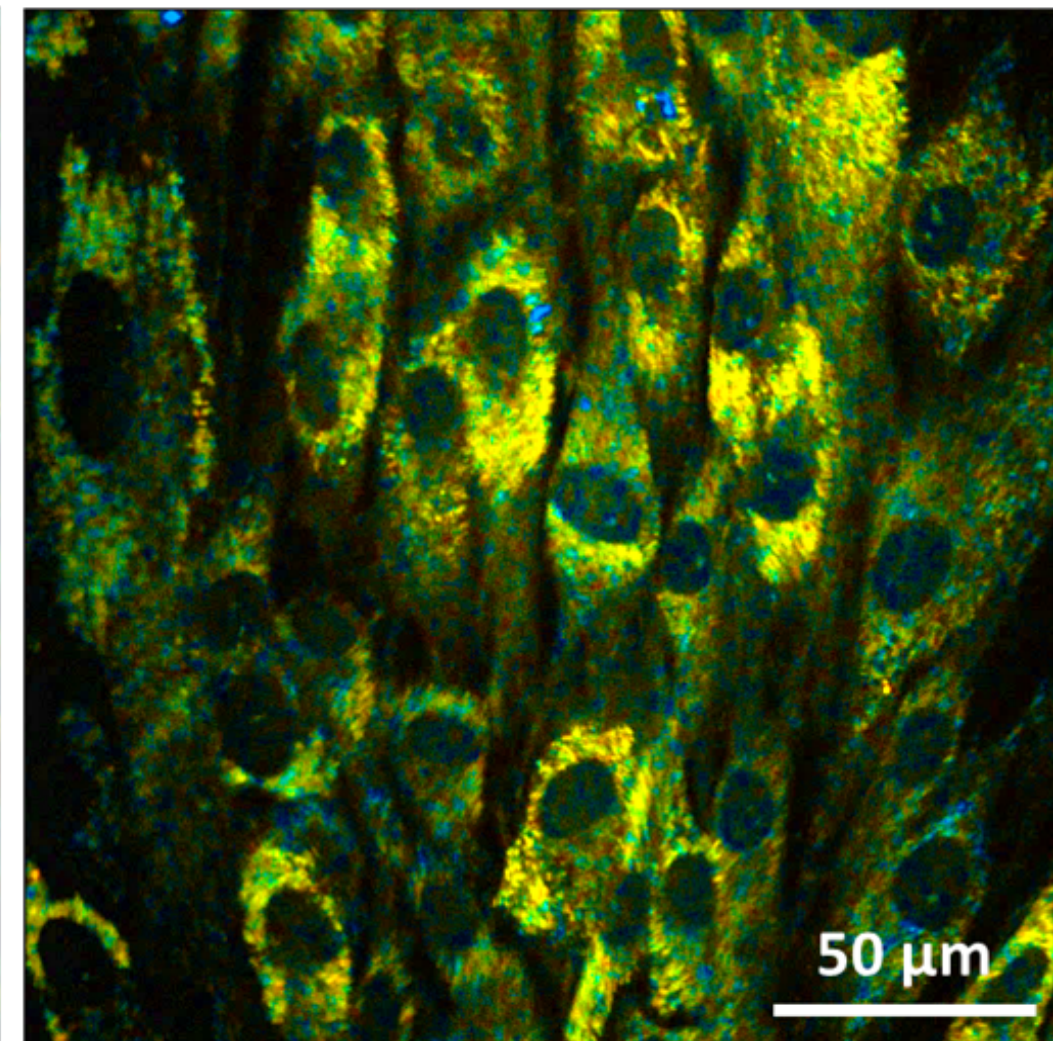
848 48. Chen, B. et al. Sensing and imaging of mitochondrial viscosity in living cells by a red
849 photoluminescent probe with long lifetime. *Chemical Communications*. **55**, 7410 (2019).

850 49. Shen, B., Wang, L. F., Zhi, X., Qian Y. Construction of a red emission BODIPY-based probe for
851 tracing lysosomal viscosity changes in culture cells. *Sensors and Actuators B: Chemical*. **304**,
852 127271 (2019).

853 50. Chen, T., Chen, Z., Liu, R., Zheng, S. NIR fluorescent probe for detection of viscosity and
854 lysosome imaging in live cells. *Organic and Biomolecular Chemistry*. **17**, 6398 (2019).

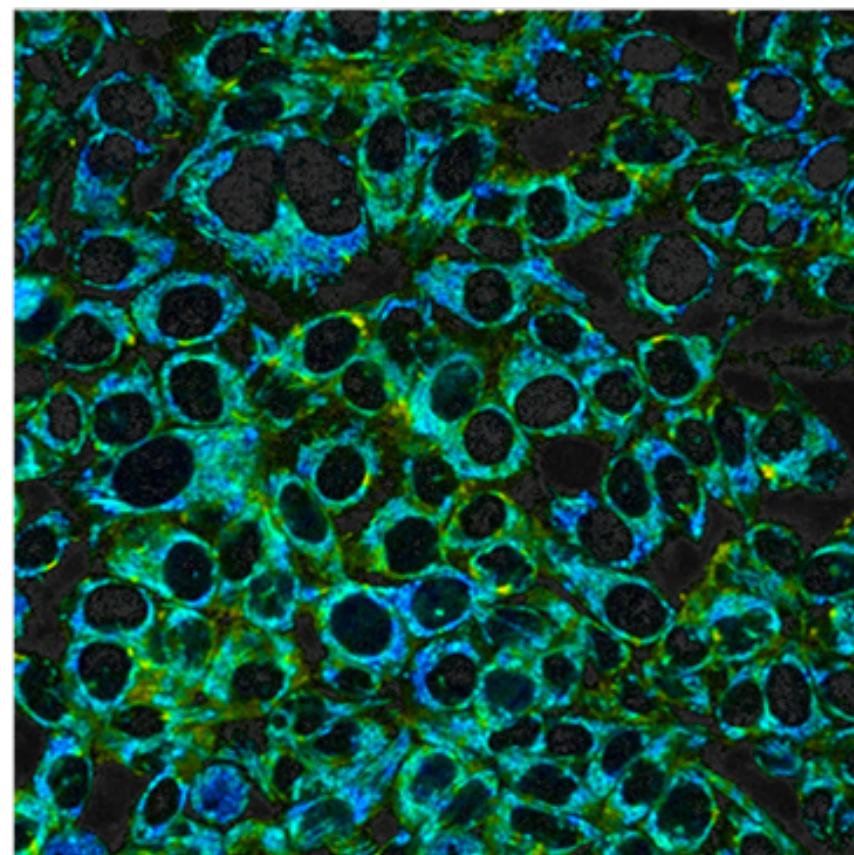
855 51. Angelucci, C. et al. Epithelial-stromal interactions in human breast cancer: effects on
856 adhesion, plasma membrane fluidity and migration speed and directness. *PLoS One*. **7** (12),
857 e50804 (2012).



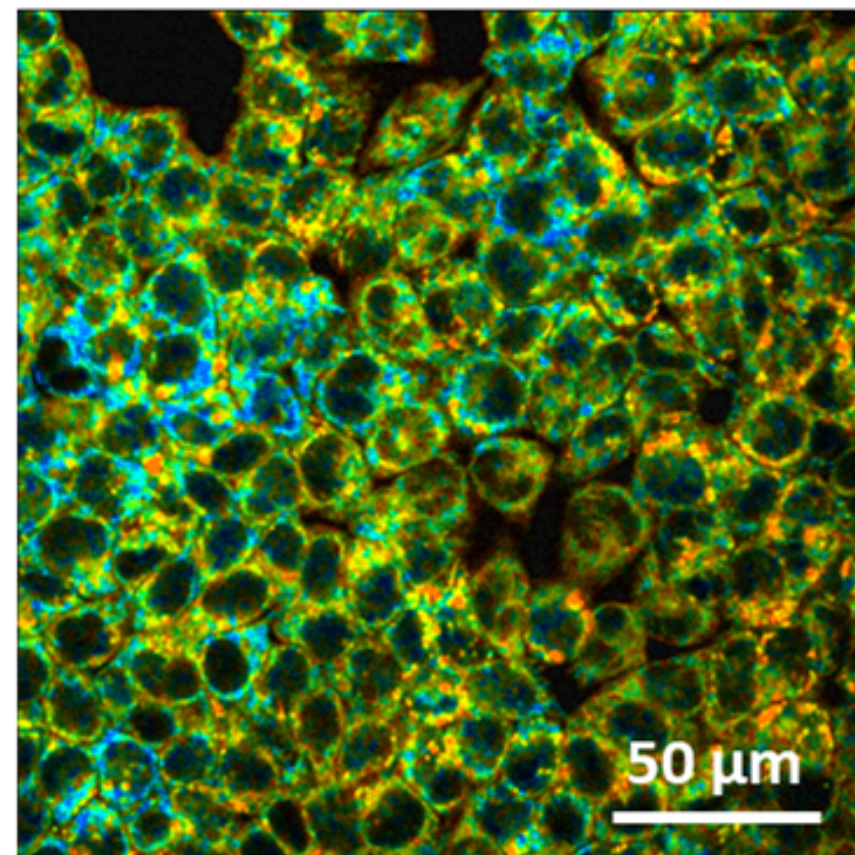
HCT116**CT26****huFB****%****75** **a_1** **40**

A

Control, 0 h



5-FU, 24 h

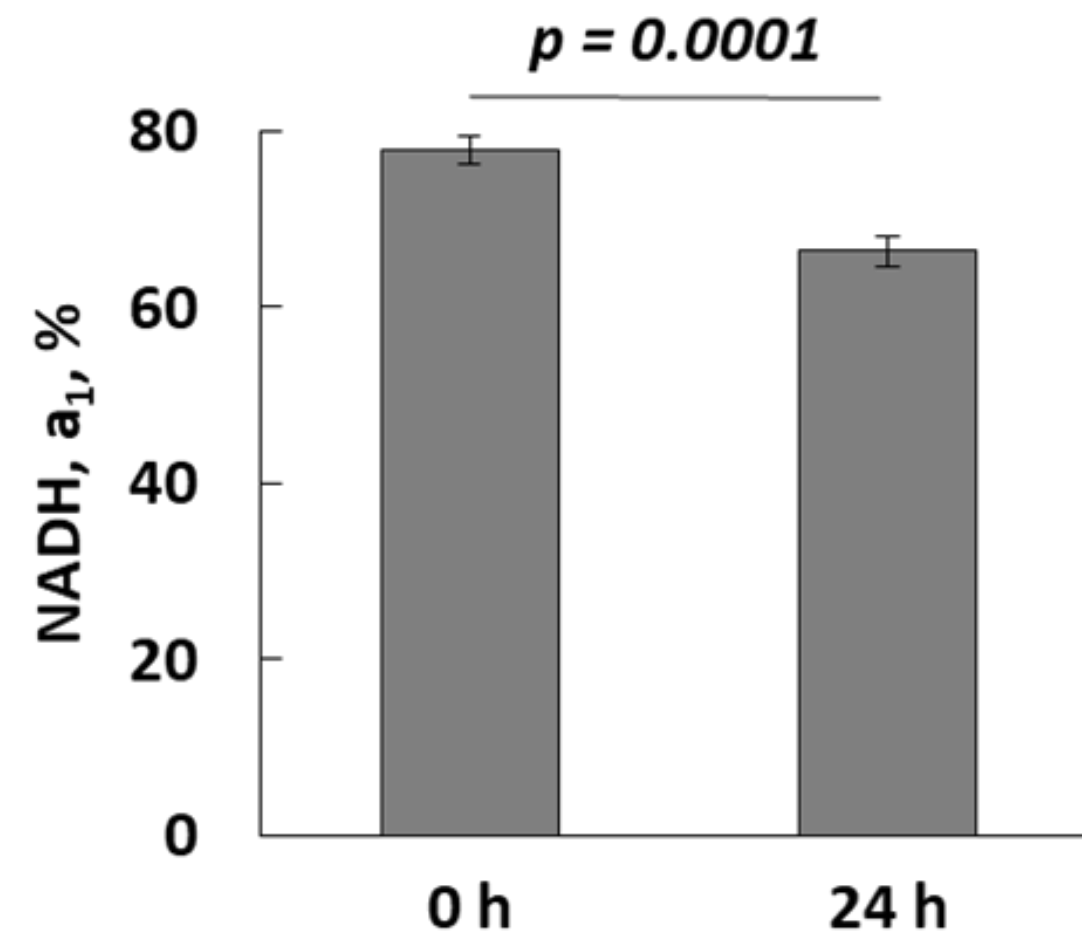


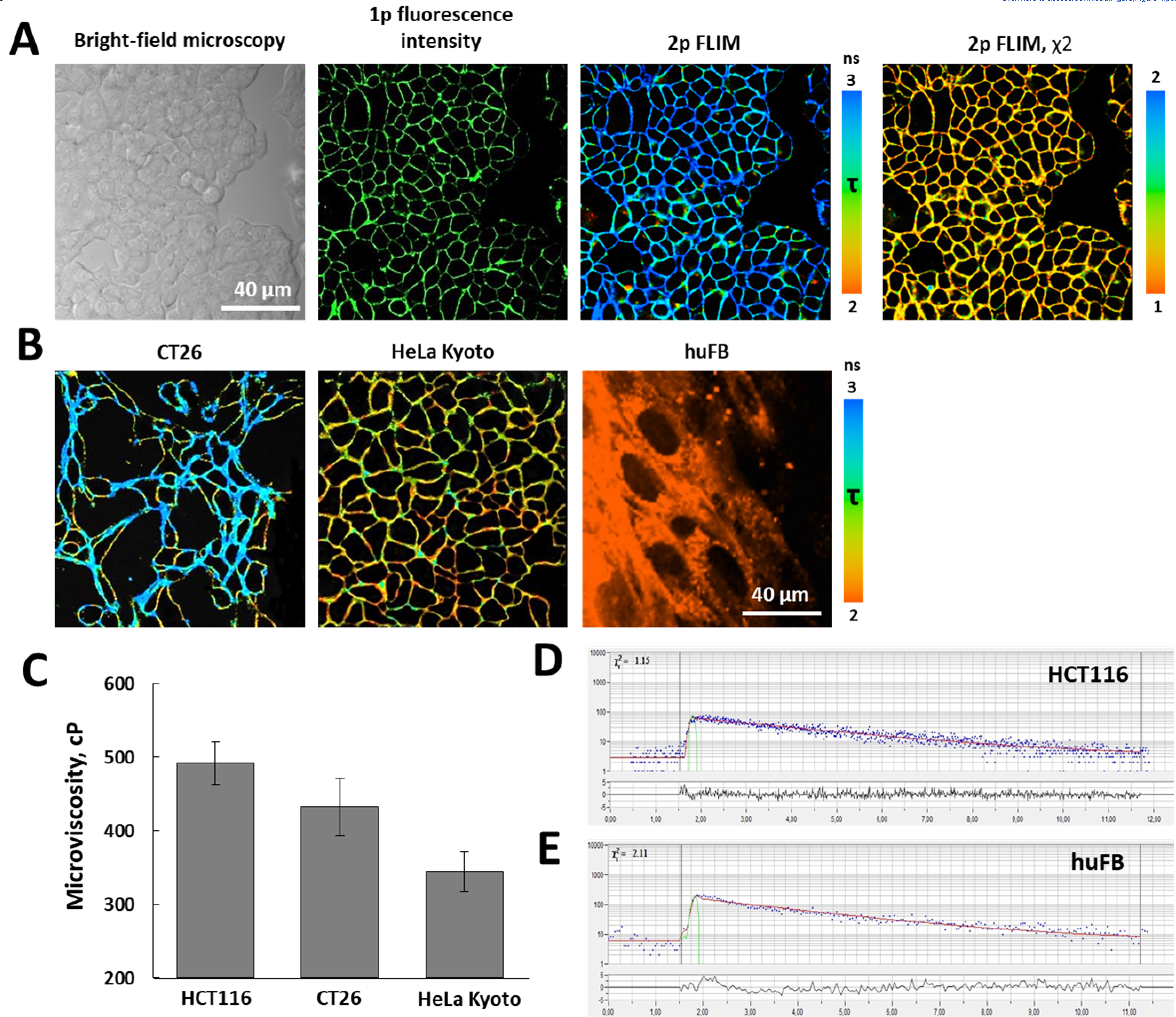
%

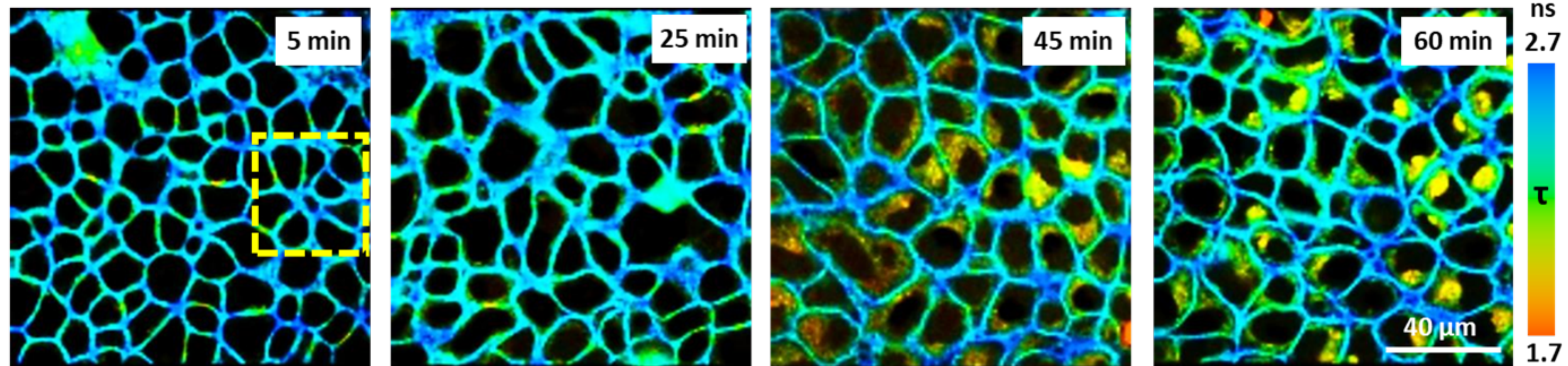
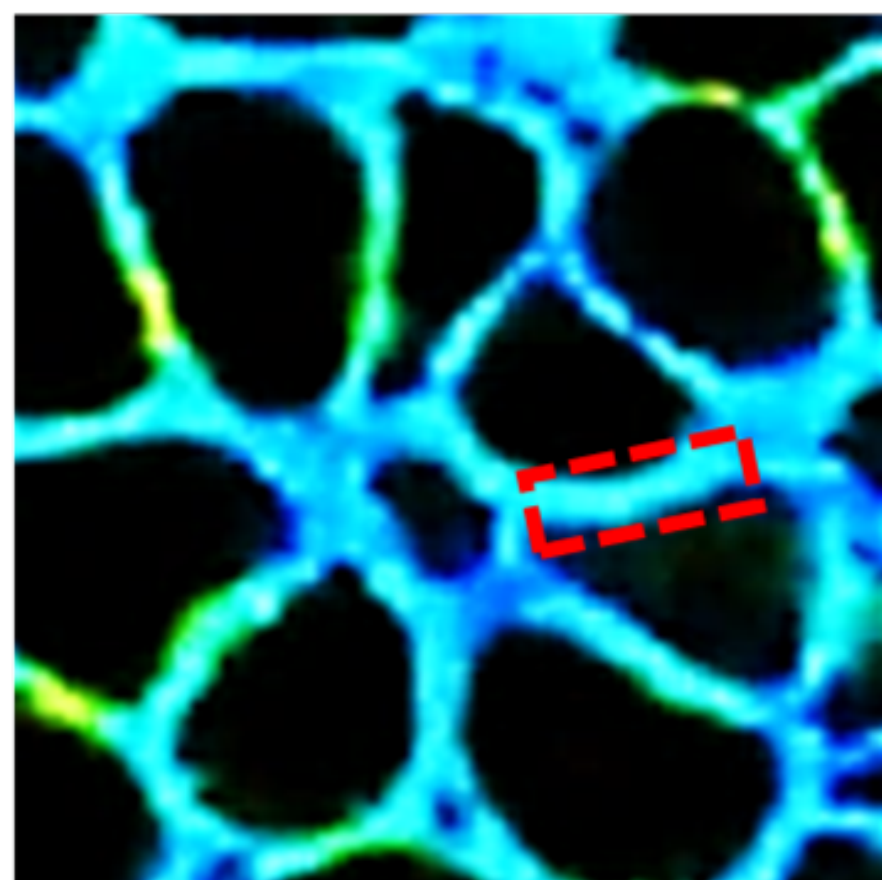
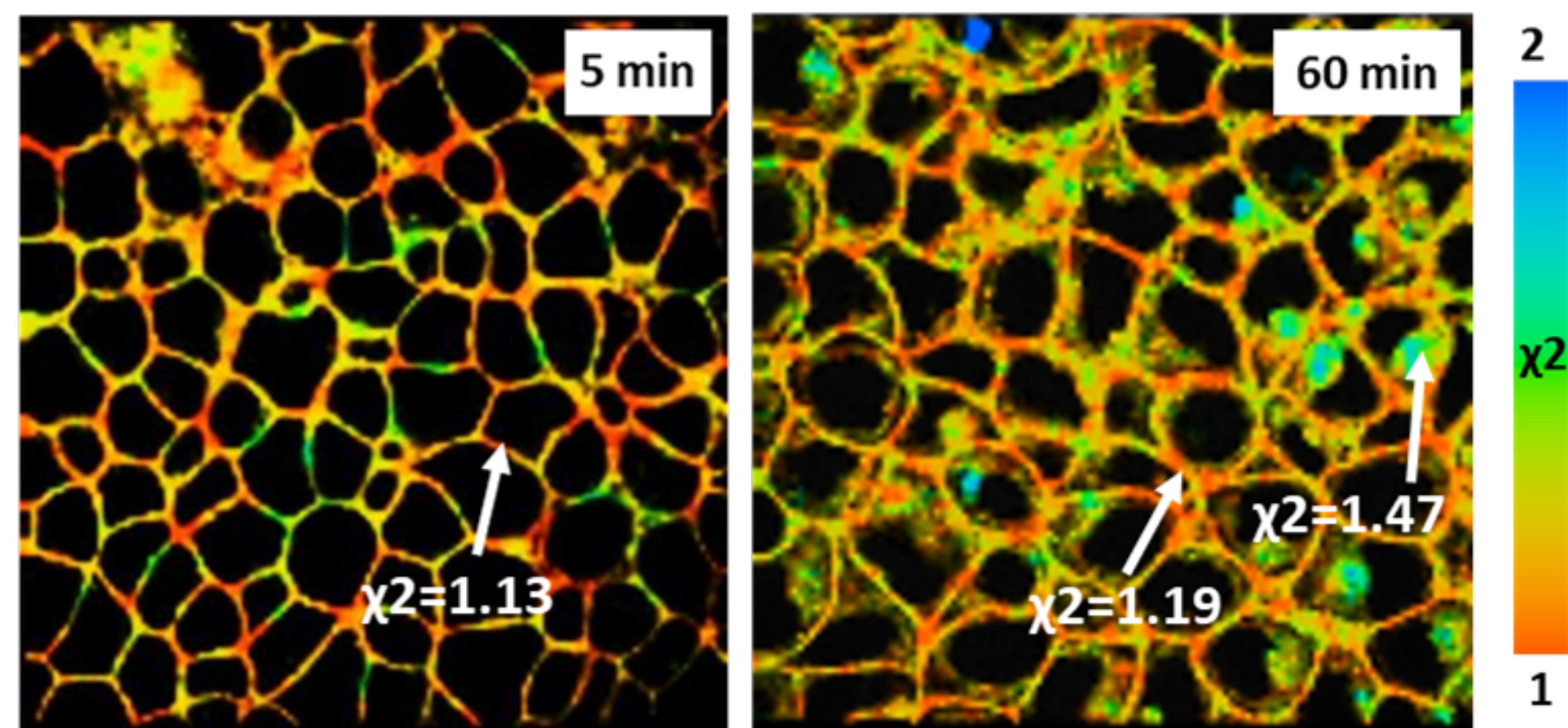
75

a₁

45

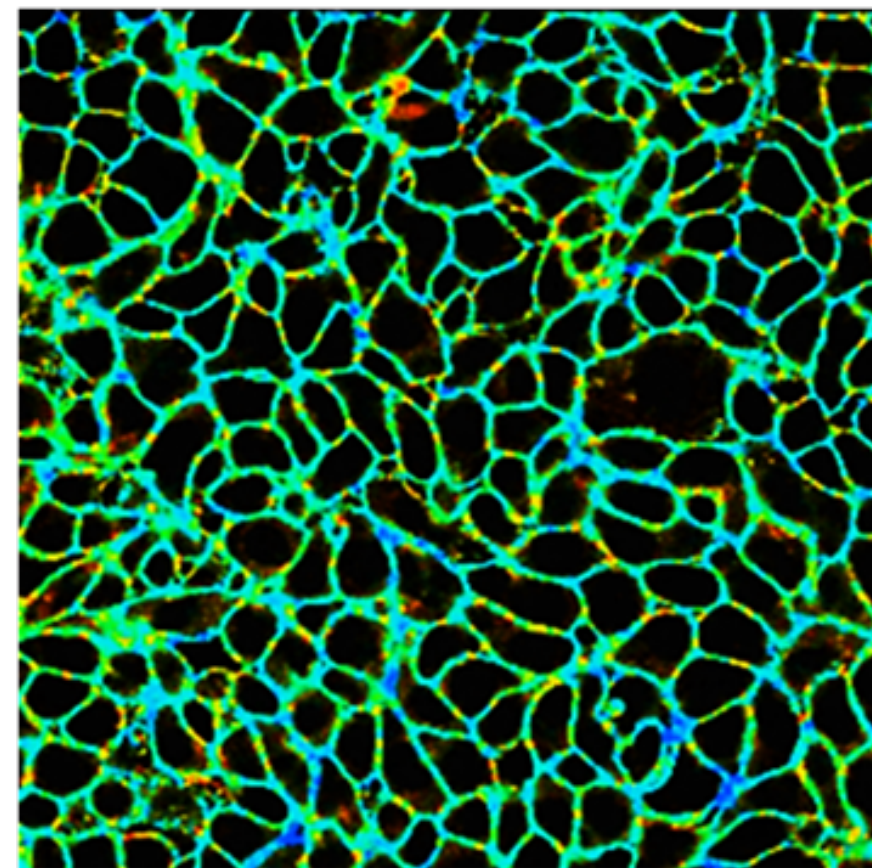
B



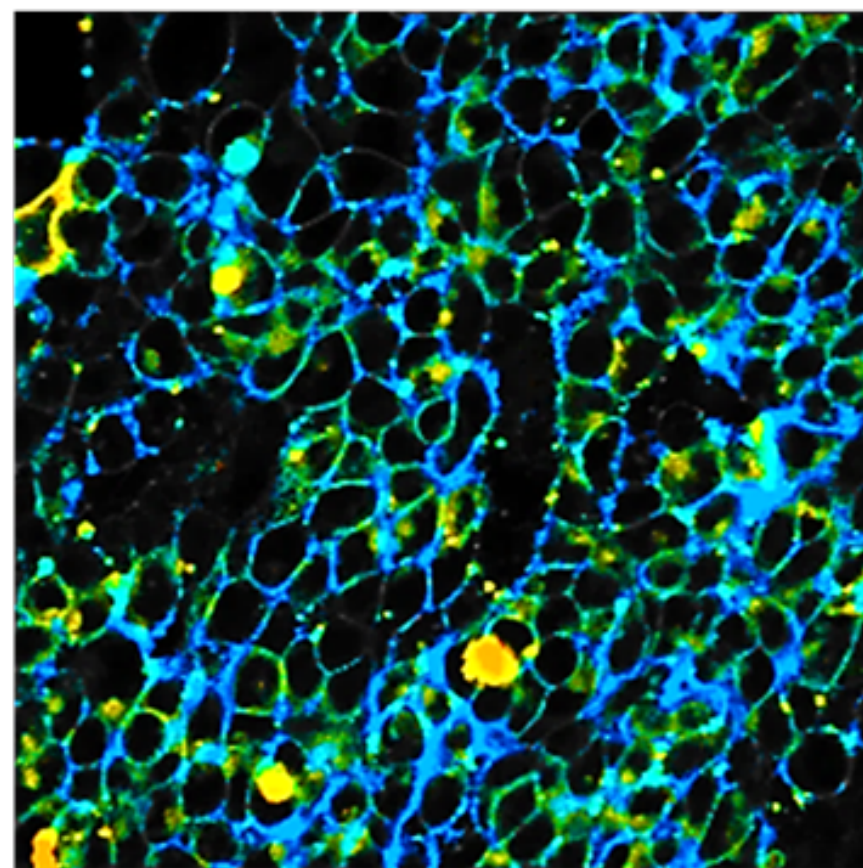
A**B****C**

A

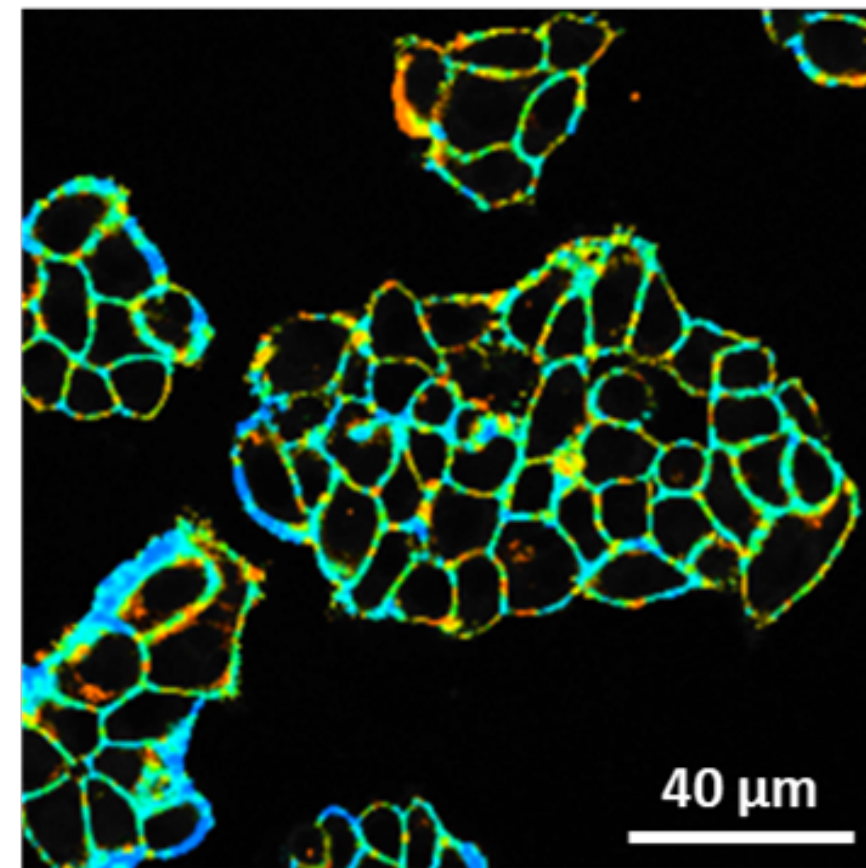
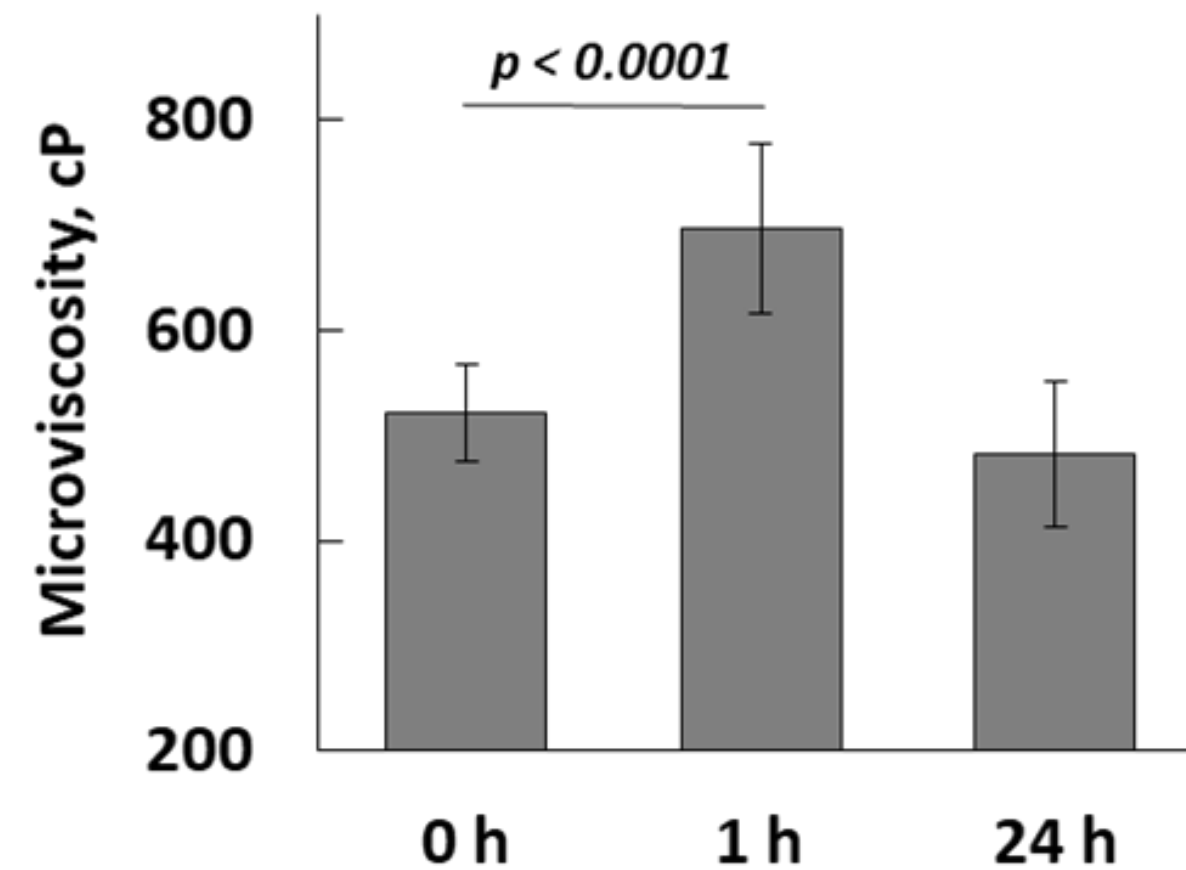
Control, 0 h



5-FU, 1 h



5-FU, 24 h

ns
3.5
 τ
2.5**B**

	NADH			
Cell line	τ_1 , ns	τ_2 , ns	a_1 , %	a_2 , %
HCT116	0.55±0.06	2.55±0.11	74.74±1.83	25.26±1.83
CT26	0.53±0.03	2.51±0.09	77.18±2.06	22.82±2.06
HeLa Kyoto	0.52±0.05	2.61±0.21	76.41±1.85	23.59±1.85
huFB	0.51±0.05	2.47±0.38	78.36±4.17	21.64±4.17
	FAD			
HCT116	0.38±0.03	1.97±0.14	80.86±4.19	19.14±4.19
CT26	0.36±0.03	2.01±0.08	85.01±1.65	14.99±1.65
HeLa Kyoto	0.39±0.04	2.01±0.09	86.01±2.14	13.99±2.14
huFB	0.37±0.03	2.11±0.19	81.82±3.51	18.18±3.51



[Click here to access/download](#)

Table of Materials
Shirmanova_Table of Materials.xls



We thank the Editor and the Reviewers of *JoVE* for their time and due diligence in thoroughly evaluating our manuscript "Probing metabolism and viscosity of cancer cells using fluorescence lifetime imaging microscopy." The reviewer comments have helped us to improve the clarity of our manuscript and provide additional information. In the revision, the changes are marked in **blue** in the main text. We hope that our revised manuscript is now acceptable for publication in the journal.

Editorial and production comments:

Changes to be made by the Author(s) regarding the written manuscript:

1. Please take this opportunity to thoroughly proofread the manuscript to ensure that there are no spelling or grammar issues.
2. Please specify the cells used in the protocol.

Response: We have specified the cells used in the protocol

The performance of the protocol is demonstrated using HCT116 (human colorectal carcinoma), CT26 (murine colon carcinoma), HeLa (human cervical carcinoma) and huFB (human skin fibroblasts) cells.

Reviewers' comments:**Reviewer #1:**

Manuscript Summary:

This is a very interesting and timely manuscript. Given the raising interest for FLIM-based applications, Shirmanova et al provide the community with a robust protocol for the assessment of up to three metabolic parameters: NADH, FAD and viscosity.

The manuscript is well written, the pipeline of image acquisition and analysis is clear and the images are convincing.

Major Concerns:

I have some considerations/advice for the authors which could further improve their (very good) manuscript.

1. Introduction: the authors talk about the fluorescence intensity ratio of NADH and FAD. Why is FLIM advantageous to estimate these metabolites? Why shouldn't we just limit ourselves to the ratio?

Response: We thank the Reviewer for the valuable comment. We have added the following text in the Introduction.

Although the redox ratio presents a simpler metric, compared with fluorescence lifetime, in terms of the data acquisition, FLIM is advantageous to estimate NADH and FAD, because fluorescence lifetime is an intrinsic characteristic of the fluorophore and almost not influenced by such factors as excitation power, photobleaching, focusing, light scattering and absorption, especially in tissues, unlike the emission intensity.

2. The authors are using a Zeiss setup for their analyses. This appears only later in the manuscript, and it is not obvious from the beginning. I would recommend adding a section before beginning the protocol on describing the minimal setup to perform these experiments. Not every lab has a Zeiss setup like the one described here, and most likely any 2P system with FLIM detectors would work. The authors should aim at generalizing the approach as extensively as possible.

Response: We thank the Reviewer for this recommendation. The section "Description of the minimal setup to perform FLIM" has been added in the beginning of the protocol. Adding a FLIM system to a confocal microscope requires several things: a pulsed laser, typically a ps or

fs, with the synchronization signal, a fast photon counting detector and photon counting electronics, an available output and input ports for the detector and the laser, respectively, on the microscope, and the scan clock pulses from the microscope scan controller. There is one more important thing, the scan head of the microscope must have the laser beam combiners and the main dichroic beam splitters suitable for the wavelength of the FLIM laser.

Some confocal microscopes, such as the Zeiss LSM 710/780/880 family, Leica SP8, SP5, Nikon A1, Olympus FV3000, are available with pulsed one-photon excitation sources (ps diode lasers and a tunable fiber laser) and with a confocal output port. These systems are fully compatible with FLIM.

When the microscope is equipped with the fs laser source, then two configurations are possible. One is to use a non-descanned detection. The NDD beamsplitter is usually placed in the filter carousel of the microscope and then a lens in the NDD beam path projects a demagnified image of the microscope objective on the detector. A practical advantage of the NDD in combination with multiphoton excitation is that the scanner is far less complicated than for confocal detection. There is no need for exactly cancelling the beam motion for different wavelengths, scan fields, or objective lenses. It is also not necessary to focus the fluorescence in a diffraction-limited size pinhole, and keep the alignment stable when filters or dichroic mirrors are replaced. The second configuration for FLIM with multiphoton microscope is to use a descanned detection. The advantage over the non-descanned detection is that the pinhole rejects daylight and optical reflections and slightly improves the spatial resolution. Using a confocal pinhole in combination with the two-photon excitation may also help to suppress spurious fluorescence light if there is a highly fluorescence layer close to the image plane. The disadvantage is fluorescence photons scattered in the way out of the sample are not detected. Descanned detection therefore does not exploit the deep-tissue imaging capability of multiphoton excitation.

1. Description of the minimal setup to perform FLIM

To perform the experiments described in the manuscript, the setup should meet the following requirements:

1. An inverted confocal microscope.
2. A pulsed laser, typically a ps or fs, with the synchronization signal.
3. A fast photon counting detector (time response 150 ps) and photon counting electronics.
4. An available output and input ports for the detector and the laser, respectively, on the microscope.
5. The scan clock pulses from the microscope scan controller.
6. The scan head of the microscope with the laser beam combiners and the main dichroic beam splitters suitable for the wavelength of the laser used for FLIM.
7. If two-photon excitation is used for FLIM, the NDD port in the microscope is desired.
8. For mammalian cell studies, especially for long-term experiments, the CO₂ incubator is recommended.

In our protocol, FLIM is realized using LSM880 (Carl Zeiss, Germany) system equipped with Power-Tau 152 module with the detector HPM-100-40 (Becker&Hickl, Germany) and Ti:Sapphire femtosecond laser Mai Tai (Spectra Physics, USA).

3. The cell concentrations and media conditions are cell-dependent. If the readers aim at choosing different cells, these numbers and conditions may vary. Could you add some general comments on what parameters to consider to adapt cell concentrations, and whether a more

universal media as PBS supplemented with serum can also be used if cells cannot be cultured in DMEM?

Response: We thank the Reviewer for the valuable comment. The following NOTE has been added in the Protocol section 2.

NOTE: The cell concentrations and media conditions are cell-dependent. The number of cells for seeding and cultivation time should be adapted to obtain 70-80% confluence in the microscopic dish. Different culture media can be used for imaging; the important thing is to avoid phenol red in the medium adequate for the cells, when preparing cells for microscopy.

4. Please consider indicating how to evaluate if photobleaching events occur, and what pixel binning values to aim for

Response: We thank the Reviewer for the valuable comment. We have made some clarifications in the text.

To evaluate photobleaching effects, one has to follow the photon count rate during the measurements. Typically, if the drop in the count rate exceeds 10% of the initial value, photobleaching takes place.

A binning factor 1-2 is used for NAD(P)H in cells at the indicated settings.

In the present protocol, a binning factor 3-4 is used for flavins in cancer cells and 2-3 - in fibroblasts.

5. Can you suggest any alternative method to apply if the FAD intensity is too low to calculate lifetime? Or provide the name of cell lines where FAD cannot be imaged so your readership is aware of potential problems ahead? Could this limitation be also setup-dependent?

Response: We have revised the text of the NOTE in section 3.

NOTE: Due to specifics of metabolism, fluorescence intensity of flavins in cancer cell lines is typically lower than in normal cells (e.g. fibroblasts or mesenchymal stem cells). Therefore, the analysis of fluorescence lifetime in cancer cells requires applying the pixel binning to adjust the number of photons to ≥ 5000 . In the present protocol, a binning factor 3-4 is used for flavins in cancer cells and 2-3 - in fibroblasts.

6. Please consider adding whether you should open and weigh BODIPY powder in a sterile environment, and how long can the stock solution be kept in the fridge once resuspended.

Response: We thank the Reviewer for the valuable comment. We agree that it is necessary to open and weigh BODIPY powder in a sterile environment. The creators of the molecular rotor claim that the stock solution can be stored in a refrigerator at +4°C for several months. We have added these clarifications in the protocol (section 4.2 and NOTE)

Open and weigh BODIPY 2 powder in a sterile environment.

Once resuspended, it can be stored in the refrigerator for several months.

7. Chapter 3, step 6: Are these physically the same cells as before or independent samples? If so, do you switch the microscope temperature controller off as the last step or as the first one? This is a key step as you need to wait until the microscope reaches 18°C, and add BODIPY accordingly not to overincubate it. The timeline here should be better detailed.

Response: We have added some clarifications in the protocol Section 4

1. The cells are imaged in BODIPY 2 solution without washing at room temperature (~20 °C) to slow down internalization of the rotor. The temperature-controlled stage of the microscope should be switched off in advance, i.e. before BODIPY 2 is added to the cells. For our setup, cooling of the stage takes about 10 min.

8. To calculate fluorescence ratio, can you please provide a main method with the commands to follow in ImageJ and at least an alternative one for the non-familiar reader?

Response: The text has been extended and NOTE has been added

NOTE: Alternatively, fluorescence intensities of NAD(P)H and FAD in cells can be measured using standard software of the microscope and the redox ratio can be obtained by dividing these values in Excel.

9. Can the authors provide a comparative experiment where viscosity is altered (another chemical etc...) in Fig. 6, that would allow the reader to have a direct comparison among conditions? What is the extent of changes in viscosity that one should expect before differences can be considered significant?

Response: We thank the Reviewer for the valuable comment. We have added additional image and the data in Figure 6, and revised the text accordingly.

Minor Concerns:

1. Line 61: time-resolved

2. Line 104: microscopic imaging is a weird formulation to me. Either use microscopy or imaging.

3. Line 146: what is a "typical" pixel? I would suggest removing this word, it is quite unclear to establish what the authors mean by this.

4. Line 249: THE corresponding (the is missing)

Response: The text has been corrected.

5. Line 252: above in the manuscript the authors reported >3000 photons as a minimal value to collect for NADH. Here 5000 is reported: which is which, then?

Response: Indeed, the minimal number of collected photons per decay curve should not be less than 3000. For adequate bi-exponential fitting, it can be adjusted to 5000 using the binning option upon data processing, if 5000 photons can not be collected by increasing laser power or image collection time. We have made some clarifications in the text on this account (section 3.11 and NOTE).

Pixel intensities should be ≥ 3000 photons per decay curve at binning 1.

For adequate bi-exponential fitting, pixel intensities should be ≥ 5000 photons per decay curve, possibly with binning. A binning factor 1-2 is used for NAD(P)H in cells at the indicated settings.

Reviewer #2:

Manuscript Summary:

In this manuscript, the authors demonstrate a method for detecting cellular metabolism and plasma membrane viscosity in live cells. The metabolism status was presented by the fluorescence of NADH, and the viscosity was measured by a sensitive dye to visualize the cancer cells changes. This manuscript is very helpful for us to understand the details of this method, while several concerns need to be addressed.

Major Concerns:

As listed in Table 1, the t_1 values were around 0.42 ns, which I believe is the peak of t_1 distribution curve. But the distribution range is also very important. The distribution curves of t_1 , t_2 , χ^2 of Figure 1B should be provided. If the range of t_1 is larger than 0.6 ns, it is improper to contribute t_1 as free NAD(P)H. Also, χ^2 values are hard to be lower than 1.20 for all the pixels in a FLIM image. Would the authors provide more details to reduce the χ^2 values or discuss the reason?

Response: Naturally, the χ^2 values may exceed 1.2 at the certain areas of the image. The reason for that is that either the fitting model is not appropriate or number of photons is so high in the specific pixel, that it is hard for the software to find a decay profile that perfectly overlays the experimental data points at every time point. In the latter case, the high χ^2 values do not mean that the analysis of the data is not accurate. Vice versa, the reduced χ^2 values in the areas with low photon numbers do not warranty a correct model used for fitting at these areas.

The distribution curves of t1, t2, χ^2 of Figure 1B have been added.

Minor Concerns:

Since NADPH has almost the same optical property as NADH, it should be clarified that the detected fluorescence is from NADPH and NADH. NAD(P)H is often used instead of NADH.

Response: Corresponding clarification has been added in the Introduction. NADH was replaced with NAD(P)H, where appropriate.

The detected fluorescence of NAD(P)H is from NADH and its phosphorylated form NADPH, as they are spectrally almost identical.

Reviewer #3:

Manuscript Summary:

Shirmanova et al presented a protocol on employing fluorescence lifetime imaging microscopy (FLIM) of endogenous fluorophores NADH and FAD along with ratiometric optical redox computation for metabolic imaging and subsequently FLIM of exogenous fluorophore BODIPY 2 for viscosity measurements in cancer cells. The authors demonstrated their protocol by imaging response of 3 cancer cells and one fibroblast cell line to chemotherapy treatment. The study did not find significant correlation between cellular viscosity and metabolic state of the cells.

Major Concerns:

1. FLIM of metabolic cofactors - A more general context would be ideal so that this would be useful for readers who use other microscope set-up, acquisitions software, FLIM analysis software.

Response: We have added the section 1 "Description of the minimal setup to perform FLIM" and several notes in the protocol to generalize it. Also, we have removed some excessive details from the parameters in the menu of SPCM software. Meanwhile, we can not avoid the details in the protocol as it will contradict the JoVE requirements ("The protocol text should provide a detailed description to enable the accurate replication of the presented method by both experts and researchers new to the field. For actions involving software usage, provide all specific details (e.g., button clicks, software commands, any user inputs, etc.) needed to execute the actions.").

1. Description of the minimal setup to perform FLIM

To perform the experiments described in the manuscript, the setup should meet the following requirements:

1. An inverted confocal microscope.
2. A pulsed laser, typically a ps or fs, with the synchronization signal.
3. A fast photon counting detector (time response 150 ps) and photon counting electronics.
4. An available output and input ports for the detector and the laser, respectively, on the microscope.
5. The scan clock pulses from the microscope scan controller.
6. The scan head of the microscope with the laser beam combiners and the main dichroic beam splitters suitable for the wavelength of the laser used for FLIM.

7. If two-photon excitation is used for FLIM, the NDD port in the microscope is desired.
8. For mammalian cell studies, especially for long-term experiments, the CO₂ incubator is recommended.

NOTE: Depending on the microscope and the laser, different objectives and laser powers can be used. For two-photon excitation, oil- or water-immersion objectives with a high numerical aperture (>1) are preferred. The laser power is selected based on the available objective but should not exceed 10 mW to avoid photobleaching and saturation issues. Image size is selected based on personal preferences.

NOTE: The parameters indicated in 9 and 14 are specific for the electronics and the detector used. If a different system is used, take care about the photon counting rate. The optimal number of collected photons per decay curve for bi-exponential fitting should not be less than 5000 (possibly with binning 3-4) at reasonable collection time (60-120 s).

2. Could the authors provide the power at the sample for 5% 750nm excitation and 9% 900nm laser powers.

Response: The average power applied to the samples was ~6 mW for both wavelengths, which corresponds to 5% 750 nm excitation and to 9% 900 nm laser powers. Corresponding clarification has been added to the text (sections 3.3 and 3.5)

3. Line 128, image size of 1024X1024 was mentioned, however, a size of 256X256 is mentioned in lines 138-142.

Response: Image size 1024X1024 pixels is used for the fluorescence intensity images, while 256x256 pixels is used for FLIM. The different image sizes are used because the obtaining of the intensity image requires less number of photons, therefore we prefer to have it more "detailed". FLIM image implies a large amount of photons in each pixel for adequate fitting. Smaller image size allows to collect the required number of photons (≥ 3000 per decay curve) for a reasonable time (60 s). In any case, image size is selected based on personal preferences, and this clarification has been added in the NOTE.

Image size is selected based on personal preferences.

4. Line 149-153 - It should be made clear that laser power should be same for all collected images for redox ratio measurements.

Response: The suggested clarification has been added in the NOTE.

NOTE: Since excitation power affects the emission intensity, laser power at the specific wavelength (750 nm or 900 nm) should be the same for all collected images for redox ratio measurements.

5. Are the authors proposing to image NADH and FAD first and then stain the cells with BODIPY 2? If so, could this be clearly stated?

Response: The NOTE about performing viscosity imaging after metabolic imaging is in the text (section 4). Additionally, we have made some revision in the Introduction.

To avoid contamination of the relatively weak endogenous fluorescence with fluorescence of the BODIPY-based rotor, imaging of the same layer of cells is performed sequentially with fluorescence of NAD(P)H and FAD imaged first.

6. Data Analysis, line 235, how can the authors be certain that background is same for all images. If this is not the case, subtracting the value from NADH and FAD would affect this intensity-based measurement. The redox ratio might be falsely high or low depending on background and not due to metabolism.

Response: In our studies on intensity-based imaging background does not change much because all the experiments are performed in identical conditions (no ambient light, no fluctuations of the laser power, the same filters and detectors used). To account for possible (small) changes of the background, it is subtracted from the intensity images.

7. Details on ImageJ functions (or tools) used for redox ratio calculation and cytoplasm selection would be helpful.

Response: The text has been corrected

8. Line 252, do the authors remove background from the images before fitting? If not, binning should be carefully used since the pixels in near the boundaries of cells would be binned with background pixels. Also, it should be mentioned that binning would decreasing resolution.

Response: In SPCImage the fitting model does include the background correction.

The text about the binning has been revised.

Keep in mind that large binning decreases image resolution.

9. There is no mention of collecting IRF(instrument response function) during imaging or its use in lifetime fitting. This is an important part of FLIM fitting and should be discussed.

Response: In a laser scanning system it is difficult, if not impossible, to measure an IRF. The excitation wavelength is usually blocked by filters, and a fluorophore with sufficiently short lifetime is not available. In multiphoton microscopy recording of an SHG signal is an option but also this is not free of pitfalls. The SHG is emitted in forward direction and only partially scattered

back into the detection beam path. This can broaden the recorded signal or distort it by reflections from the trans-illumination light path. SPCImage therefore provides several ways to avoid IRF recording altogether. An IRF is calculated from the rising edge of the fluorescence decay curves in the FLIM data. The calculation is run on the combined data of several pixels around the brightest spot in the image. The IRF obtained this way is reasonably correct when the recorded signal is fluorescence with a lifetime several times longer than the width of the IRF. Systematic deviations can occur when SHG or an extremely fast fluorescence decay component are present, or when the rising edge is distorted by laser leakage. Although the use of recorded IRFs is not recommended for reasons described above SPCImage is able to run the FLIM analysis with real IRF data. The IRF can either be derived from an independent FLIM data file or from the FLIM data themselves. The latter option is convenient for multiphoton tissue FLIM data. These often contain a substantial amount of SHG signal. For this case, one has to select a region which is dominated by SHG, declare the waveform of this area an IRF, and run the data analysis with this IRF.

The NOTE about IRF has been added in the protocol.

NOTE: IRF (Instrument Response Function) is an important part of FLIM fitting. In SPCImage IRF is automatically calculated from the rising edge of the fluorescence decay curves. Meanwhile, IRF can be recorded using non-fluorescent sample, e.g. ceramics, or a sample that produces SHG (Second Harmonic Generation) signal, e.g. collagen, urea crystals or sugar. The use of the recorded IRFs is not recommended if there is an option to calculate it in the software.

10. From figures 1D, 4 D and 4E, the values T1 and T2 (the black vertical bars set at the beginning and end of the decay) in SPCImage is set to different values. Ideally these should be consistently used. Please explain how these were set.

Response: We thank the Reviewer for the valuable comment. Figure 4D has been replaced with the figure that was obtained with the same setting as Figure 4E. The position of the first black line (time channel from which the analysis is started) is determined by the settings in the SPCImage software and it is normally set to the time of the rising edge of the decay. The time channels that are located on the left side of the black bar are used for the calculation of the background. The right bar is normally set to the position where the decay curve approaches the background.

11. Please provide reference for the fact about NADPH compared to NADH stated in line 446-447.

Response: Reference 37. Blacker, T. S., Mann, Z. F., Gale, J. E., Ziegler, M., Bain, A. J., Szabadkai, G., & Duchon, M. R. Separating NADH and NADPH fluorescence in live cells and tissues using FLIM. *Nature Communications*. 5, 3936 (2014) **is in the body of the manuscript.**

Additional reference has been added: 38. Lu, W., Wang, L., Chen, L., Hui, S., Rabinowitz, J.D. Extraction and Quantitation of Nicotinamide Adenine Dinucleotide Redox Cofactors. *Antioxid Redox Signal*, 28(3), 167-179 (2018).

Minor Concerns:

1. Line 207, check grammar

2. Please include the versions of the SPCImage and Zen software used on the table of materials.

Response: The versions of the software have been added in the Table of Materials.

3. Table of materials, last two rows, some fields are not in English.

Response: The text of the table has been revised.

Reviewer #4:

This is an interesting and well written manuscript that includes a detailed description of how to use FLIM to probe the cellular metabolism and plasma membrane viscosity in cancer cells in vitro. The authors describe how to avoid contamination of the relatively weak endogenous fluorescence with fluorescence of the BODIPY-based rotor. The authors also explain how to collect the fluorescence lifetimes of the cofactors in the cytoplasm, and the fluorescence lifetime of the rotor in the plasma membranes of cells by manual selection of corresponding zones as regions of interest. The authors apply this protocol to correlate metabolic state and viscosity for different cancer cell lines and to assess the changes after chemotherapy.

Minor comments

- The authors mention that they are probing "simultaneously cellular metabolism and plasma membrane viscosity in cancer cells in vitro by FLIM". However, they mention that to avoid contamination of the relatively weak endogenous fluorescence with fluorescence of the BODIPY-based rotor, imaging of the same layer of cells is performed sequentially. Therefore, the authors should avoid the word simultaneous to describe this approach.

Response: We agree with the Reviewer and have replaced the word "simultaneous" with "sequential"

- The authors do not specify the cells used in protocol (section 1) but then suggest the use of DMEM when using medium without phenol red. The authors should mention that the important thing is to avoid phenol red in the medium adequate for the cells, when preparing cells for microscopy imaging.

Response: We thank the Reviewer for the valuable comment and have added the clarifications about the cells and cell culture

The performance of the protocol is demonstrated using HCT116 (human colorectal carcinoma), CT26 (murine colon carcinoma), HeLa (human cervical carcinoma) and huFB (human skin fibroblasts) cells.

NOTE: The cell concentrations and media conditions are cell-dependent. The number of cells for seeding and cultivation time should be adapted to obtain 70-80% confluence in the microscopic dish. Different culture media can be used for imaging; the important thing is to avoid phenol red in the medium adequate for the cells, when preparing cells for microscopy.

- This sentence "In order to monitor cells in the same microscopic fields of view in dynamics, use glass bottom dishes with a lined bottom for the cells seeding" should be clarified. Right now it's difficult to understand the authors' meaning.

Response: The sentence has been revised.

In order to monitor cells in the same microscopic fields of view in dynamics, use **gridded glass-bottom dishes** for the cells seeding.

- The authors suggest the use of the following settings in laser scanning microscope (section 2): the excitation wavelengths in two-photon mode 128 750 nm, the registration range 450-490 nm, laser power 5 %, image size — 1024 × 1024 129 pixels, pixel size 0.42 μm, bit depth—16-bit. The authors should include a note that 5% power may need adjustment to avoid photobleaching or saturation issues. Same comment for "laser power 9 %".

Response: The note has been included in the Protocol.

The laser power is selected based on the available objective and should be adjusted to avoid photobleaching and saturation issues.

- Authors need to describe the microscopy instrument used in the experiments. They obviously are using a Zeiss microscope but there should be a detailed description of the microscope used so readers can understand how the experiments are performed.

Response: The section 1 "Description of the minimal setup to perform FLIM" has been added in the Manuscript. Detailed information about the microscope is in the Table of Materials.

- Section 2-10, as they indicate to scan the sample 60 s, they should also mention the photons collected (or events measured) as that would be more appropriate for readers to follow in their own instruments and applications

Response: The details about collected photons have been added in the NOTE.

5000 photons per decay curve (binning 1) are typically collected at the photon counting rate $1-2 \times 10^5$ photons/s.

- Improve readability: "In the case, if further increase of the laser power or image collection time is impossible due to cell damage, use the pixel binning by clicking the Bin option in SPCImage software for data processing."

Response: The text has been revised.

If further increase of the laser power or image collection time is impossible due to morphological alterations (an indicator of a cell damage) or photobleaching, use the pixel binning by clicking the *Bin* option in SPCImage software for data processing.

- Temperature conditions for section 3-6 need to be clarified. Why are rotor measurements performed at room temperature considering that membrane viscosity is affected by temperature?

Response: We thank the Reviewer for the valuable comment. We agree that temperature is a critical parameter for membrane viscosity and in the range 20-37 °C the fluctuations in viscosity are significant for several cell lines studied [17,18]. Imaging of the rotor in cells was performed at room temperature in order to slow down the penetration of the rotor into the cell (i.e. slow down endocytosis). This allows imaging of viscosity for up to 30 minutes. At higher temperature (37 °C), the molecular rotor enters the cell very quickly, which complicates the measurements in the plasma membrane. Temperature conditions have been clarified in the text (section 4.1).

The cells are imaged in BODIPY 2 solution without washing at room temperature (~20 °C) to slow down internalization of the rotor. We note that membrane viscosity is temperature dependent, as demonstrated in our previous work.

- Authors need to explain what Ti:Sa laser is and again this can be addressed by adding a section on the confocal microscope used as an example so readers can adapt their own instruments.

Response: The section 1 “Description of the minimal setup to perform FLIM” has been added in the Manuscript.

- Section 5-2 provide a better statistical analysis of background subtraction

Response: All the experiments were performed in identical conditions (no ambient light, no fluctuations of the laser power, the same filters and detectors used), which allowed to avoid the background fluctuations. To account for possible (small) changes of the background, it is subtracted from the intensity images. The details about the subtraction procedure in ImageJ have been added in the protocol (sections 6.2 and 6.4).

Highlight a cell-free area in the NAD(P)H image using a circle or a square option, calculate the background signal using command *Measure*, write down the resulting value in the field *Subtract* (select *Process* on the main panel, then *Math* and *Subtract*).

Obtain the image of the optical redox ratio by dividing the FAD fluorescence intensity by NAD(P)H fluorescence intensity (select *Process* on the main panel, then *Image Calculator* and select *Divide*, check the box *Create new window* and press *OK*).

- Provide references for the different equations that can be used to calculate the optical redox ratio, e.g. NADH/FAD or FAD/(FAD+NADH).

Response: We have added references

- Be consistent about "Adjust binning to achieve pixel intensities of ≥ 5000 photons per decay curve". Previously authors suggested minimum limit of 3000 photons for when binning should be performed. Also connecting time collecting FLIM data should be connected to the number of photons per decay curve

Response: Indeed, the minimal number of collected photons per decay curve should not be less than 3000 for the fluorophores with bi-exponential decays. For adequate bi-exponential fitting, it can be adjusted to 5000 using the binning option upon data processing, if 5000 photons can not be collected by increasing laser power or image collection time. 5000 photons per decay curve (binning 1) are typically collected at the photon counting rate $1\text{--}2 \times 10^5$ photons/s.

We have made some clarifications in the text on this account (section 3.11 and NOTE)

- IRF use should be addressed. Are authors using automated version provided by SPCI?

Response: Please, see the answer to the question 9 of the Reviewer 3. The NOTE about IRF has been added.

NOTE: IRF (Instrument Response Function) is an important part of FLIM fitting. In SPCImage IRF is automatically calculated from the rising edge of the fluorescence decay curves. Meanwhile, IRF can be recorded using non-fluorescent sample, e.g. ceramics, or a sample that produces SHG (Second Harmonic Generation) signal, e.g. collagen, urea crystals or sugar. The use of the recorded IRFs is not recommended if there is an option to calculate it in the software.

- Representative results section is a bit confusing to read. Readability needs to be improved.

Response: The text of the Results section has been revised.

- Figure 1b needs scale bar. Are all the figure panels from the same area of sample? Can the cells' images be compared?

Response: Scale bar has been added in Fig. 1B. The images of the intensity and redox ratio have been replaced with correct ones, obtained from the same cells.

- Figure 2 CT26 image shows some damage to the cells and it should be replaced

Response: FLIM image of CT26 cells in Fig. 2 has been replaced.

Video Produced by Author: Less than 50 MB. If your video is greater than 50 MB, click "offline" as the delivery method and our

This piece of the submission is being sent via mail.